

# Rule Generation for Classification: Scalability, Interpretability, and Fairness

Tabea E. Röber<sup>a</sup>, Adia C. Lumadjeng<sup>a</sup>, M. Hakan Akyüz<sup>b</sup>, Ş. İlker Birbil<sup>a</sup>

<sup>a</sup>University of Amsterdam, 11018 TV, Amsterdam P.O. Box 15953, The Netherlands

<sup>b</sup>Erasmus University Rotterdam, 3000 DR, Rotterdam, The Netherlands

**ABSTRACT:** We introduce a new rule-based optimization method for classification with constraints. The proposed method leverages column generation for linear programming, and hence, is scalable to large datasets. The resulting pricing subproblem is shown to be NP-Hard. We recourse to a decision tree-based heuristic and solve a proxy pricing subproblem for acceleration. The method returns a set of rules along with their optimal weights indicating the importance of each rule for learning. We address interpretability and fairness by assigning cost coefficients to the rules and introducing additional constraints. In particular, we focus on local interpretability and generalize separation criterion in fairness to multiple sensitive attributes and classes. We test the performance of the proposed methodology on a collection of datasets and present a case study to elaborate on its different aspects. The proposed rule-based learning method exhibits a good compromise between local interpretability and fairness on the one side, and accuracy on the other side.

*Keywords:* Machine Learning; Linear Programming; Rule Generation; Interpretability; Fairness

---

**1. Introduction** Classification is a supervised learning problem that assigns categorical labels, *e.g.*, classes, to a target variable within a provided dataset. Decision trees and decision rules are two related techniques commonly used in machine learning for classification tasks. A decision tree corresponds to a type of supervised learning algorithm that creates a tree-like model of decisions and their possible consequences. The tree is constructed by recursively partitioning the data into smaller subsets, based on the value of a feature, until the leaf nodes contain (almost) homogeneous subsets of the target variable. Decision rules, on the other hand, are sets of if-then statements that describe how the values of the input variables are used to determine the value of the target variable. These rules can be useful for gaining insights into the relationships among variables and for making predictions based on those relationships. One can consider a decision tree as a collection of dependent decision rules since every leaf node of a decision tree corresponds to a decision rule.

In various application areas decision rules are considered to be interpretable by the decision makers. Such a rule consists of one or more conditions, and these conditions designate a class when all of them are satisfied. For example in binary classification, “**if (Last payment amount is less than 100) and (Months since issue date is less than 90) then the credit risk is good**” is a rule that can be used to predict the credit risk of customers. When a sample satisfies this rule, then it receives a label corresponding to one of the two classes: “**good**” or “**bad**”. In case a sample is covered by more than one rule, then the majority vote among the assigned labels may be used to determine the class of the sample.

In this work, we propose a rule-learning algorithm for classification with constraints based on mathematical programming. We present a general linear programming (LP) model for generating rules for multi-class classification. One advantage of using mathematical programming over off-the-shelf libraries containing popular algorithms (*e.g.*, random forests, boosting methods, or neural networks) is its flexibility in adding specific constraints, such as those related to interpretability and fairness. Integrating such constraints in traditional machine learning (ML) techniques is not straightforward.

Bertsimas and Dunn (2017) also emphasize this point and suggest that mathematical programming is highly flexible in solving ML problems. However, state-of-the-art approaches that address classification problems by solving mixed-integer linear programming (MILP) formulations quickly become intractable when there are thousands of integer variables (Bertsimas and Dunn, 2017; Aghaei et al., 2021; Alston et al., 2022). This significantly limits the practical use of MILPs for large datasets. Therefore, our motivation is to develop an LP-based approach that is both scalable enough to handle large datasets and flexible enough to incorporate constraints.

In our approach, each rule corresponds to a column in the mathematical programming model. When dealing with a large number of rules, our algorithm utilizes the column generation (CG) procedure to obtain the rules iteratively. This feature also connects our method to an earlier LP-based learning method, LPBoost by Demiriz et al. (2002). LPBoost solves an LP that is similar to ours and learns using weak learners within a CG procedure. In that sense, our approach can be considered as a tailored LPBoost framework that is designed for decision rules considering interpretability and fairness aspects. Nevertheless, as we highlight in the following, our rule generation framework is different from the literature.

First, the LPBoost is characterized for binary classification problems. The works by Gehler and Nowozin (2009) and Saffari et al. (2010) attempt to adapt the LPBoost into a multi-class setting, and both studies put in extra constraints. Saffari et al. (2010) build the LP formulation using a constraint for each sample-class pair similar to *one-versus-rest* approach. In addition to extra terms and additional constraints, Gehler and Nowozin (2009) also modify the constraints of the LPBoost. However, neither approach scales well, as adding an additional constraint per sample per class increases the computational burden of multi-class LPBoost. Our approach directly addresses multi-class classification without the need to define new constraints or resorting to *one-versus-rest* approach. Second, every weak learner of the LPBoost casts a vote for each sample in the constraints. Nonetheless, working with rules forces one to work with only a subset of the dataset. Our approach resolves this by associating each sample with a subset of rules for classification resulting in a sparser formulation. Third, prior studies mentioned above primarily focus on accuracy performance and do not consider interpretability and fairness. Our method stands out by explicitly addressing these aspects which make it a more comprehensive approach for multi-class classification.

Overall, the contributions of this work can be summarized as follows:

- (i) We offer a new rule-learning algorithm that is based on an LP formulation, making it scalable for large datasets. This provides a significant advantage compared to existing studies that use MILP formulations.
- (ii) To the best of our knowledge, our work is the first to demonstrate that the resulting pricing subproblem to find a rule is NP-hard. As a remedy, our rule generation approach allows the use of a regular decision tree with sample weights as the pricing subproblem. Training trees with sample weights is both very fast and standard in most off-the-shelf ML libraries. Combining such a rule generation approach with solving the pricing subproblem quickly increases scalability even further.
- (iii) Our methodology directly addresses multi-class problems while existing studies using optimization-based approaches are developed for binary classification. This also eliminates additional efforts of solving the MILPs repetitively in a *one-versus-rest* approach as in existing works.
- (iv) In addition to a set of rules and their associated costs, our LP model also provides the optimal rule weights. These weights can be used to assign importance to each rule and are critical to locally interpret the resulting classification made for individual observations.
- (v) We introduce two metrics that address multiple classes and multiple protected groups for group fairness based on avoiding disparate mistreatment. These metrics are easily placed as constraints in our general LP model.
- (vi) We demonstrate the use of our proposed algorithm in a case study, and conduct numerical experiments to compare its performance against other mathematical optimization-based classifiers. Our results show that our algorithm is highly accurate and more scalable than other methods. To ensure reproducibility, we provide access to the implementation of our proposed algorithm through a dedicated public repository.

**2. Related Literature** The literature on mathematical optimization-based approaches (MOBAs) to solve classification problems is very rich. Therefore, we confine ourselves to the studies using decision trees (DTs) and rule-based methods that are most relevant to our proposed method. We refer to the works by Gambella et al. (2021), Carrizosa et al. (2021) and Ignatiev et al. (2021), which provide excellent overviews of MOBAs for classification.

**Scalability.** MILP formulations are prominent in rule-based learning on which our methodology also relies. Malioutov and Varshney (2013) propose a rule-based binary classifier by solving an integer program that minimizes the number of rules for a boolean compressed sensing problem. Wang and Rudin (2015) present a MILP formulation to collect decision rules for binary classification. Dash et al. (2018) use a CG-based framework to find an optimal rule set for binary classification, where the objective is to balance the simplicity of classification rules and the algorithm’s accuracy. For large instances, the pricing subproblem is either solved with time limits, or the columns are generated by a greedy heuristic. Wei et al. (2019) propose generalized linear rule models for binary classification using a similar CG framework as in Dash et al. (2018). Malioutov and Meel (2018) solve a MaxSAT formulation by constraint programming to construct interpretable classification rules. Ghosh and Meel (2019) also propose a framework based on MaxSAT formulation that can be applied to binary classification problems with binary features to minimize the number of generated rules and the number of misclassified samples.

Decision rules (or rule sets) show similarity with DTs in the sense that every leaf node of a DT can be translated into a single rule by following the decision path starting from the root node. Bertsimas and Dunn (2017) aim to find an optimal DT for classification by formulating a MILP problem where single and multi-dimensional half-spaces recursively divide the feature space into disjoint areas during its construction. Verwer and Zhang (2019) propose a MILP formulation based on binary encoding of features to learn optimal DTs with a predefined depth. McTavish et al. (2022) introduce a method for fast sparse decision tree optimization via smart guessing strategies applicable to any optimal branch-and-bound-based decision tree algorithm. Other notable works considering DTs include Firat et al. (2020); Aghaei et al. (2021); Günlük et al. (2021); Alston et al. (2022), and Demirović et al. (2022). These studies depend on solving MILPs or enumerative search strategies, and thus, suffer from intractability on large datasets due to their long-running time requirements. Alternatively, our methodology is based on an LP formulation to achieve scalability.

**Interpretability.** To address interpretability, the MOBAs above mostly rely on the comprehensibility of shallow DTs or simplicity of rules to human understanding. The latter is often considered easier to understand than a DT, since even a moderate-depth DT can be relatively complex (Fürnkranz, 1999). Many studies directly address interpretability, for example aiming to induce sparsity and limit the number of rules (*e.g.*, Lakkaraju et al., 2016; Wang et al., 2017, 2019; Guidotti et al., 2018; Bertsimas et al., 2019; Blanquero et al., 2019; Proença and van Leeuwen, 2020; Lawless et al., 2023; Yang and van Leeuwen, 2022). This perspective is also called *global* interpretability by Molnar (2022). Although global interpretability can provide insight into the characteristics of the data in general, it is of limited practical usage when individualized recipes are to be provided at the sample level. The latter is termed *local* interpretability (Molnar, 2022) and relevant to recommend patient-specific medical recipes or loan application approval of consumers that require individualized explanations. Unlike the existing MOBAs mentioned, we concentrate on local interpretability to fill the gap in the literature.

**Fairness.** Fairness is often formulated using additional constraints to avoid discrimination over disadvantaged groups in the data and receives growing attention in the MOBAs literature. Lawless et al. (2023) extend the rule learning framework of Dash et al. (2018) to take into account fairness for binary classification. Likewise, Jo et al. (2022) incorporate different group fairness notions by modifying the MILP formulation from Aghaei et al. (2021) for binary classification. We generalize fairness notions beyond binary classification to encompass

multiple classes and also extend them to involve multiple sensitive attributes.

**3. Mathematical Programming Models** Consider a training dataset  $\mathcal{D} = \{(\mathbf{x}_i, y_i) : i \in \mathcal{I}\}$  for a classification problem, where  $\mathcal{I}$  is the index set of samples,  $\mathbf{x}_i \in \mathbb{R}^d$  and  $y_i$  denote the vector of features and the label of sample  $i \in \mathcal{I}$ , respectively. We define a rule as a conjunction of conditions that partitions the feature space of the samples. These conditions are often called as *literals* in Boolean formulae literature for concept learning, and the rule itself corresponds to a *term* in a Disjunctive Normal Form (DNF) (see Rivest, 1987; Kearns et al., 1994). The main idea of the proposed learning approach is to obtain a set of rules indexed by  $\mathcal{J}$  and the corresponding nonnegative rule weights  $w_j$ ,  $j \in \mathcal{J}$  so that the prediction for each sample is given as a *weighted* combination of the rule predictions. A sample  $i \in \mathcal{I}$  is covered by a rule  $j \in \mathcal{J}$  if and only if the sample satisfies all conditions in the rule. To this end, we construct LP models that minimize the total loss and the overall cost of using the rules. As we shall see next, working with LP models gives us an invaluable advantage for scaling our approach to much larger datasets and considering multi-class problems. Moreover, we can easily extend our models with additional constraints in our training process without any need for pre- or post-processing of input or output data.

The subsequent segment of this section consists of four parts. We first introduce in Subsection 3.1 the master problem that is used for the classification problem. Subsection 3.2 elucidates the rule generation scheme used for the column generation (CG) procedure. The resulting pricing subproblem structure of the CG, its complexity, and our proxy pricing subproblem approach are presented in Subsection 3.3. Finally, we devote Subsection 3.4 to addressing the interpretability and incorporating fairness constraints into our model.

**3.1 Master Problem** Suppose that the problem consists of  $K$  classes. To work with multiple classes, we define a vector-valued mapping  $\mathbf{y}_i \in \mathbb{R}^K$  as in Zhu et al. (2009). That is, if  $y_i = k$ , then

$$\mathbf{y}_i = \left(-\frac{1}{K-1}, -\frac{1}{K-1}, \dots, 1, \dots, -\frac{1}{K-1}\right)^\top, \quad (1)$$

where the value one appears only at the  $k^{\text{th}}$  component of the vector. A given rule  $j \in \mathcal{J}$  assigns the vector  $\mathbf{R}_j(\mathbf{x}_i) \in \mathbb{R}^K$  to input  $\mathbf{x}_i$ , only if the rule covers sample  $i \in \mathcal{I}$ . This vector is also formed in the same manner as in (1) and represents the rule  $j$ 's prediction for sample  $i$ . The final prediction of sample  $i$  is then made using a weighted average of all rule predictions,  $\mathbf{R}_j(\mathbf{x}_i)$ 's, and their associated weights,  $w_j$ 's. Now, the prediction vector for sample  $i \in \mathcal{I}$  becomes

$$\hat{\mathbf{y}}_i(\mathbf{w}) = \sum_{j \in \mathcal{J}} a_{ij} \mathbf{R}_j(\mathbf{x}_i) w_j,$$

where  $\mathbf{w} = (w_j : j \in \mathcal{J})^\top$  represents the vector of rule weights, and  $a_{ij} \in \{0, 1\}$  indicates whether rule  $j \in \mathcal{J}$  covers sample  $i \in \mathcal{I}$  or not; *i.e.*,  $a_{ij} = 1$  or  $a_{ij} = 0$ . The predicted class of sample  $i$  is determined by assigning it to the highest element (to the corresponding class) in the prediction vector  $\hat{\mathbf{y}}_i(\mathbf{w})$ . We break ties arbitrarily, namely, we assign the class of a sample randomly among the highest value elements in its prediction vector. In order to evaluate the total classification error, we use the *hinge loss* function and define

$$\mathcal{L}(\hat{\mathbf{y}}_i(\mathbf{w}), \mathbf{y}_i) = \max\{1 - \kappa \hat{\mathbf{y}}_i(\mathbf{w})^\top \mathbf{y}_i, 0\}, \quad (2)$$

where  $\kappa = (K - 1)/K$ . Next, we introduce the auxiliary variables  $v_i$ ,  $i \in \mathcal{I}$  standing for  $v_i \geq \mathcal{L}(\hat{\mathbf{y}}_i(\mathbf{w}), \mathbf{y}_i)$ . We can conclude that a sample  $i \in \mathcal{I}$  is correctly classified when  $v_i = 0$ . However, a positive value of  $v_i$  does not necessarily imply misclassification but only gives an indication of the strength of incorrectly classifying sample  $i \in \mathcal{I}$ . This characteristic stems from employing weighted combinations of rules for sample predictions. Now, we are ready

to present the LP model of our master problem:

$$\begin{aligned}
& \text{minimize} && \lambda \sum_{j \in \mathcal{J}} c_j w_j + \sum_{i \in \mathcal{I}} v_i \\
& \text{subject to} && \sum_{j \in \mathcal{J}} \hat{a}_{ij} w_j + v_i \geq 1, && i \in \mathcal{I}, \\
& && v_i \geq 0, && i \in \mathcal{I}, \\
& && w_j \geq 0, && j \in \mathcal{J},
\end{aligned} \tag{3}$$

where  $\hat{a}_{ij} = \kappa a_{ij} \mathbf{R}_j(\mathbf{x}_i)^\top \mathbf{y}_i$  is a measure of classification accuracy of rule  $j$  for sample  $i$  given that the sample is covered by the rule, and the coefficients  $c_j \geq 0$ ,  $j \in \mathcal{J}$  stand for the costs of rules. For example, these cost coefficients can reflect the length of the rule (*e.g.*, the number of conditions used) for sparsity or they may be simply set to one. The objective function shows the trade-off between the accuracy and the cost of using rules. Since these two summation terms are in different units, the hyperparameter  $\lambda \geq 0$  is used for scaling.

**3.2 Rule Generation** The LP model (3) of our master problem operates with a given set of rules,  $\mathcal{J}$ . Notice that  $\mathcal{J}$  contains exponentially many rules due to all possible splitting combinations (namely *partitions*) of the features. The number of such partitions of the feature space based on the training dataset  $\mathcal{D}$  can be counted using *Bell numbers* (see, Liu, 2022), which grow quickly with the number of features and their associated levels. This aspect shows the combinatorial structure of the problem and prohibits us to generate the set of rules explicitly as its size becomes extremely large. Hence, we resort to an alternative way to generate the beneficial rules iteratively.

In the master problem, the rules correspond to columns, and obtaining them in an iterative scheme leads to the well-known column generation (CG) procedure in optimization (Desaulniers et al., 2006). At each iteration of this approach, an LP model is constructed with a subset of the columns (*column pool*). This model is called the *restricted master problem*. After solving the restricted master problem, the dual optimal solution is obtained. Then, using this dual solution, a *pricing subproblem* (PSP) is solved to identify the columns with negative *reduced costs*. These columns are the only candidates for improving the objective function value when they are added to the column pool. The next iteration continues after extending the column pool with the negative reduced cost columns.

In order to apply CG to our problem, we define a subset of rules  $\mathcal{J}_t \subset \mathcal{J}$  at iteration  $t$  and form the restricted master problem by replacing  $\mathcal{J}$  with  $\mathcal{J}_t$  in our LP models. Let us denote the dual variables associated with the first set of constraints in (3) by  $\beta_i$ ,  $i \in \mathcal{I}$ . In vector notation, we use boldface font as  $\boldsymbol{\beta}$ . Then, the *dual restricted master problem* at iteration  $t$  becomes

$$\begin{aligned}
& \text{maximize} && \sum_{i \in \mathcal{I}} \beta_i \\
& \text{subject to} && \sum_{i \in \mathcal{I}} \hat{a}_{ij} \beta_i \leq \lambda c_j, && j \in \mathcal{J}_t, \\
& && 0 \leq \beta_i \leq 1, && i \in \mathcal{I}.
\end{aligned} \tag{4}$$

If we denote the optimal dual solution at iteration  $t$  by  $\boldsymbol{\beta}^{(t)}$ , then improving the objective function value of problem (4) requires finding at least one rule  $j' \in \mathcal{J}/\mathcal{J}_t$  such that

$$\bar{c}_{j'} = \lambda c_{j'} - \sum_{i \in \mathcal{I}} \hat{a}_{ij'} \beta_i^{(t)} < 0, \tag{5}$$

where  $\bar{c}_{j'}$  is also known as the *reduced cost* of column  $j'$ . In fact, this condition simply checks whether  $j' \in \mathcal{J}/\mathcal{J}_t$  violates the dual feasibility. To find those rules with negative reduced costs, we formulate the pricing subproblem for classification as

$$\min_{j' \in \mathcal{J}/\mathcal{J}_t} \left\{ \lambda c_{j'} - \sum_{i \in \mathcal{I}} \hat{a}_{ij'} \beta_i^{(t)} \right\}. \tag{6}$$

Note that the second term measures the *weighted* classification error for all those points



classified by rule  $j \in \mathcal{J}/\mathcal{J}_t$ . The weight for each sample  $i \in \mathcal{I}$  is given by the corresponding dual optimal solution,  $\beta_i^{(t)}$ . We will use this observation to devise a method to solve our PSP.

When the PSP does not return any rule with a negative reduced cost, then we have the optimal solution to the master problem with the current set of rules,  $\mathcal{J}_t$ . Otherwise, we have at least one rule with a negative reduced cost. After adding one or more rules with negative reduced costs to  $\mathcal{J}_t$ , we proceed with  $\mathcal{J}_{t+1}$  and solve the restricted master problem or, equivalently, its dual (4). It is important to note that the sole purpose of solving the PSP is to return a subset of rules with negative reduced costs.

**3.3 Pricing Subproblem** We formulate the PSP stated in (6) as a binary integer linear program (BILP). To that end, we focus on the case where we have a target class  $k \in \mathcal{K}$  to predict and it is possible to consider each class in a *one-versus-rest* setting without loss of generality. At first glance, it might seem to be a simplification to formulate the PSP as a binary classification problem using *one-versus-rest* instead of directly modelling it as a multi-class problem. There are two primary reasons for this choice. First, the multi-class problem requires introducing extra integer variables to represent the classes associated with a rule. Second, the multi-class problem leads to a nonlinear integer formulation. As shown in the subsequent, we take advantage of two classes (*one-versus-rest*) to fix a rule's prediction as positive for the target (*i.e.*, positive) class, and thus, represent the PSP as a BILP. Observe that *one-versus-rest* setting can be achieved in polynomial time considering each class  $k \in \mathcal{K}$ . Similarly, we devise a one-hot encoding scheme as described in the works by Hastie et al. (2009) and Dash et al. (2018). The features are transformed into a binary form. For categorical features, a binary variable per category and their negations are created indicating whether a sample belongs to a category or not. For numerical features, threshold values corresponding to the deciles of the dataset  $\mathcal{D}$  are used to define binary variables similarly (for further details see Dash et al., 2018). The dataset  $\mathcal{D}$  is also represented using such a binarization of features that can be achieved in polynomial time of the dataset size. We should emphasize that our LP framework is generic and the master problem (3) does not necessitate the discretization of features. Here, our aim is to provide a comprehensive analysis of the PSP and to show theoretical properties associated with its structure.

Before delving into the details of the PSP formulation, we first introduce some additional notation. For simplicity, we remove the iteration index  $t$  and the rule index  $j$  from the PSP formulation as we are seeking an optimal rule  $j^*$ . Let  $a_i$  and  $s_p$  represent binary variables taking a value of one when sample  $i \in \mathcal{I}$  is covered by the rule and feature  $p \in \mathcal{P}$  is included in the rule, respectively, and zero otherwise. Here,  $\mathcal{P}$  stands for the set of features after binarization. The parameter  $x_{ip}$  has a value of one when sample  $i$  satisfies feature  $p$  and zero otherwise. The samples  $i \in \mathcal{I}$  are divided into two subsets as  $\mathcal{I}^+$  and  $\mathcal{I}^-$  where the former set of samples has the same label with the target class  $k$  and the latter set of samples is from other classes, *e.g.*,  $\mathcal{K} \setminus \{k\}$ . Now, we can represent the label of sample  $i \in \mathcal{I}^+$  (or  $i \in \mathcal{I}^-$ ), *e.g.*, when  $y_i = k$  (or  $y_i \neq k$ ), with  $\mathbf{y}_i = (1, -1)^\top$  (or  $\mathbf{y}_i = (-1, 1)^\top$ ). Similarly, prediction  $\mathbf{R}(\mathbf{x}_i)$  of the rule for sample  $i$  becomes  $\mathbf{R}(\mathbf{x}_i) = (1, -1)^\top$  and  $\mathbf{R}(\mathbf{x}_i) = (-1, 1)^\top$  when sample  $i$  is covered,  $a_i = 1$ , and not covered,  $a_i = 0$ , respectively. Thus, omitting the rule index  $j^*$ ,  $\hat{a}_i$  in (6) for sample  $i$  reduces to  $\hat{a}_i = \kappa a_i \mathbf{R}(\mathbf{x}_i)^\top \mathbf{y}_i = a_i$  for  $i \in \mathcal{I}^+$  and  $\hat{a}_i = -a_i$  for  $i \in \mathcal{I}^-$ . We take the inverse of (6) and the PSP is presented as follows:

$$\begin{aligned}
& \text{maximize} && \sum_{i \in \mathcal{I}^+} a_i \beta_i - \sum_{i \in \mathcal{I}^-} a_i \beta_i - \lambda \sum_{p \in \mathcal{P}} (1 - s_p) \\
& \text{subject to} && a_i + \sum_{p \in \mathcal{P}} (1 - s_p) x_{ip} \geq 1, && i \in \mathcal{I}, \\
& && a_i - s_p \leq 1 - x_{ip}, && i \in \mathcal{I}, p \in \mathcal{P}, \\
& && a_i \in \{0, 1\}, && i \in \mathcal{I}, \\
& && s_p \in \{0, 1\}, && p \in \mathcal{P}.
\end{aligned} \tag{7}$$

The objective function simultaneously maximizes the weighted number of samples from class

$k$  and minimizes the weighted number of samples from other classes covered by the rule while minimizing the number of conditions in the rule. Notice that,  $c = \sum_{p \in \mathcal{P}} (1 - s_p)$  in the third term is the associated cost of rule that counts the number of conditions (*i.e.*, rule length or number of literals) used for classification. Also, observe that, when binarization of the data is performed, each category (or a split value for numerical features without loss of generality) is associated with two binary variables: one to define a category of a feature and the other for its negation (see Dash et al., 2018). Then, a condition is only defined when either the binary variable for the category or for its negation is selected by the model. Otherwise, the rule either satisfies that category for all samples or covers no samples, and thus, there is no condition at all. Therefore, the number of conditions in a rule is calculated by simply counting the binary variables that are not selected in the formulation. The third term in the objective becomes constant and can be ignored when each rule has the same cost, *e.g.*,  $c = 1$ , if rule length is not important. The first constraint set enforces the sample to be covered by the rule when the second term on the left-hand side is zero for all features. Otherwise, the first constraint set is redundant. This implies that sample  $i$  is covered, *e.g.*,  $a_i = 1$ , if and only if there is no case a necessary feature  $p$  is not selected for  $i$ . The second constraint set complements this and enforces  $a_i = 0$  when  $s_p = 0$  and  $x_{ip} = 1$  for some feature  $p$  which is sufficient to conclude that the sample is not covered by the rule. The last two constraint sets impose binary restrictions on the variables.

It is possible to derive optimality bounds on the (3) based on the reduced cost expression in (6). Let  $z^*$ ,  $\bar{z}$ , and  $z_k^*$  denote, respectively, the optimum objective value of the master problem (3), the best objective value found so far for the master problem (3), and the optimum value for the PSP (7) solved to find a rule for class  $k$ . Note that, (7) is solved  $K$  times once for each class  $k = 1, \dots, K$  to generate rules to add in the master problem. Then, the following proposition provides a lower bound  $z_{LB}$  on  $z^*$ .

PROPOSITION 3.1  $z_{LB} = \bar{z} - \max_{k=\{1, \dots, K\}} \{z_k^*\}$  is a lower bound on  $z^*$ .

The proof follows from LP duality and thus omitted here.  $Z_{LB}$  can be used to terminate the CG procedure when a specified level of optimality gap is attained. Theoretically, the PSP has to be exactly solved at least  $K$  times (once per class) during the column generation algorithm to find an optimal solution for the master problem (3). However, as we argue next, solving the PSP exactly is not a good strategy for devising in a machine learning algorithm. The PSP is very difficult to solve as it is combinatorial in nature. Actually, Proposition 3.2 shows that our PSP is NP-hard. Therefore, the required computational effort may hamper our motivation to obtain a fast method.

PROPOSITION 3.2 *The PSP in (7) is NP-hard.*

The proof of Proposition 3.2 is given in Appendix A. The following corollary is a direct implication of Proposition 3.2.

COROLLARY 3.1 *Constructing an optimal classification rule is NP-hard.*

The proof directly follows when we set  $\beta_i = 1$  for each sample  $i \in \mathcal{I}$ . Having observed these caveats, we next devise a heuristic approach that makes use of the weighted classification structure of PSP in (7). We coin this heuristic as *proxy PSP*, which is based on growing decision trees with sample weights that correspond to the dual optimal variables. After constructing the tree, we visit each leaf of the tree and check whether the resulting rule has a negative reduced cost. The following lemma shows that indeed the samples that are misclassified would receive a positive sample weight via the dual optimal solution. The proof of the lemma is skipped, since it is based on basic LP duality theory.

LEMMA 3.1 Suppose  $v_i^{(t)}$ ,  $i \in \mathcal{I}$  are the optimal solutions of the restricted master problem at iteration  $t$ . Then, we obtain for all  $i \in \mathcal{I}$  that

$$v_i^{(t)} > 0 \implies \beta_i^{(t)} = 1 \quad \text{and} \quad \beta_i^{(t)} = 0 \implies v_i^{(t)} = 0.$$

Figure 1 shows the proposed heuristic approach for rule generation. The procedure `DecisionTree` takes a vector of sample weights as an input and returns a set of rules  $\bar{\mathcal{J}}$  (leaves of the decision tree) that satisfy (5). The subset  $\bar{\mathcal{J}}$  thus contains those rules with negative reduced costs. Similarly, the initial rule pool, denoted by  $\mathcal{J}_0$ , is generated by training a decision tree using unit weights (denoted with `DecisionTree(e)` for the samples in the upper-left part of Figure 1. When we have a set of rules without such a tree structure, it might be that a sample is not covered by any rule. However, the rules obtained from a decision tree guarantee that every (test or training) sample is covered by exactly one rule. Thus, our CG initialization scheme is likely to prohibit having uncovered samples. In case a test sample is not covered, then we resolve this issue by assigning each uncovered sample to a default class like many rule-based models; see for instance, Fürtkranz (1999); Lawless et al. (2023). Training decision trees with sample weights as such boils down to solving a *proxy pricing subproblem*. Fortunately, decision trees with sample weights can be grown extremely fast using standard ML libraries.

The essence of our rule learning framework is its flexibility to incorporate rule costs and additional constraints while maintaining scalability. In the subsequent sections, we demonstrate two such cases where interpretability and fairness concepts can be modeled. Interpretability is addressed by taking advantage of the rule weights and their associated costs. Fairness is handled by using constraints within our LP formulation.

**3.4 Interpretability and Fairness** An interpretable learning method can be considered as global or local (Molnar, 2022). The former emphasizes an explanation of the underlying model, whereas the latter focuses on individual or per-sample explanations. For example, a model with a few number of rules can be good for global interpretation. In contrast, the average number of rules per sample could be used for local interpretation, *e.g.*, for personalized explanations or recommendations. In this case, the total number of rules might not be as important as it is in global interpretation. In fact, local interpretability is usually overlooked by existing studies where the emphasis is given to global interpretation (Lawless et al., 2023; Dash et al., 2018; Wang et al., 2017; Wei et al., 2019). These studies implicitly assume that producing a few rules would make their approaches more interpretable. This can be correct from a global interpretation perspective. However, this also presumes that the same set of rules are to be used to explain the underlying reasoning behind every decision. Consider, for instance, explaining the rejection decisions for loan applications using

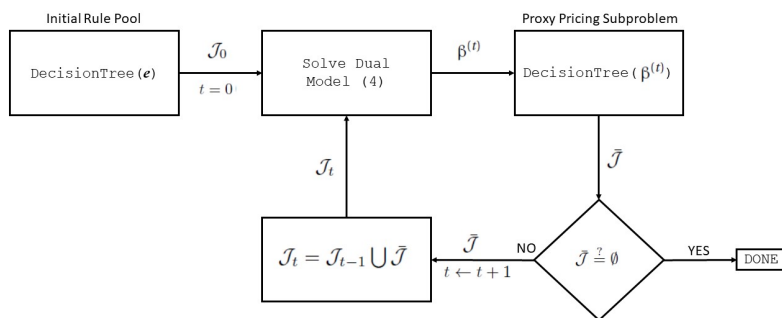


Figure 1: Proposed rule generation algorithm. The notation  $\mathbf{e}$  stands for vector of ones.



the same set of rules to all individuals. Rejected people might expect individualized and specific explanations to be able to change their status in the future. A similar deduction can be made to treat patients using individualized recipes, where local interpretation becomes highly desirable. In addition, we also consider the average rule length per sample as an indicator for local interpretability at the sample level.

Recall that our work is centered around local interpretability instead of global. However, our rule generation algorithm can incorporate well-known interpretability measures such as the number of rules, the length of a rule (*e.g.*, number of conditions used) and the number of covered samples by the rule (see Lakkaraju et al., 2016, for their definitions) by representing them as the costs associated with the rules at the global level. For instance, the number of conditions of a rule can be set as its cost, and then, our rule generation algorithm can be applied to choose the best possible combination of *short* rules.

Accurate or interpretable predictions do not automatically guarantee fairness. Nevertheless, interpretability is usually seen as a prerequisite to ensure fairness and mitigate bias in data (Arrieta et al., 2020). Fairness is divided into two as *individual* and *group* fairness by Barocas et al. (2023). The former emphasizes similar treatments for similar samples (individuals), and the latter prioritizes similar treatments among groups constituting sensitive attributes. In this work, we focus on group fairness.

Fairness notions are usually limited to regression and binary classification under two protected groups; *e.g.*, a sensitive attribute with two categories. Transforming fairness discussion from a binary classification setting into a multi-class classification with multiple protected groups is not straightforward (Denis et al., 2021; Alghamdi et al., 2022). For an overview on fairness notions from the literature for both binary and multi-class classification, we refer to Appendix B. We introduce two notions addressing multiple classes and multiple protected groups for group fairness that are based on avoiding disparate mistreatment: *Disparate Mistreatment per Class* (DMC) and *Overall Disparate Mistreatment* (ODM). To our knowledge, this is the first attempt to generalize fairness notions to multiple classes and multiple sensitive attributes addressing disparate mistreatment by using an in-processing technique (see Wan et al., 2023).

We map our fairness definitions for DMC and ODM into mathematical conditions such that they can be formulated as constraints within our LP model (3). Let  $\mathcal{G}$  be the set of protected groups  $g \in \mathcal{G}$  having distinct sensitive characteristics. Each sample  $i \in \mathcal{I}$  is associated with a protected group label  $G \in \mathcal{G}$  and a class label  $y \in \mathcal{K}$ . When samples  $i \in \mathcal{I}$  belong to group  $g \in \mathcal{G}$  and samples  $j \in \mathcal{I}$  belong to group  $g' \in \mathcal{G}$ , and both groups of samples share the same class label, *i.e.*,  $y_i = y_j = k$ , then the fairness criteria must hold between groups  $g$  and  $g'$ .

**Disparate Mistreatment per Class (DMC).** Disparate mistreatment requires an equal error rate among all groups  $g, g' \in \mathcal{G}$  for each class  $k \in \mathcal{K}$ . DMC is defined as follows:

$$P(\hat{y} \neq y | y = k, G = g) = P(\hat{y} \neq y | y = k, G = g'), \quad k \in \mathcal{K} \text{ and } g, g' \in \mathcal{G}, \quad (8)$$

which states that, empirically, the probability of incorrectly predicting each class  $k \in \mathcal{K}$  should be equal among the protected groups. In practice, (8) may be too strict to satisfy, and finding such a classifier under these conditions can be unrealistic. As a remedy, a certain level of unfairness  $\epsilon \geq 0$  may be permitted such that the inequalities

$$|P(\hat{y} \neq y | y = k, G = g) - P(\hat{y} \neq y | y = k, G = g')| \leq \epsilon, \quad k \in \mathcal{K} \text{ and } g, g' \in \mathcal{G} \quad (9)$$

hold, and disparate mistreatment is small. We translate the restrictions (9) into constraints that could be added to our LP model (3). Let  $\mathcal{I}_{k,g} = \{i \in \mathcal{I} : y_i = k, G = g\}$  be the set of indices designating the samples with class  $k \in \mathcal{K}$  and group  $g \in \mathcal{G}$  with cardinality  $|\mathcal{I}_{k,g}|$ . Then, the left-hand side of (9) for the DMC describes the difference between the classification errors of protected groups  $g$  and  $g'$  sharing the same class label  $k$ . Thus, to

address group fairness using DMC, we add the following set of constraints to the LP:

$$\frac{1}{|\mathcal{I}_{k,g}|} \sum_{i \in \mathcal{I}_{k,g}} v_i - \frac{1}{|\mathcal{I}_{k,g'}|} \sum_{i \in \mathcal{I}_{k,g'}} v_i \leq \epsilon, \quad k \in \mathcal{K} \text{ and } g, g' \in \mathcal{G}, \quad (10)$$

$$\frac{1}{|\mathcal{I}_{k,g'}|} \sum_{i \in \mathcal{I}_{k,g'}} v_i - \frac{1}{|\mathcal{I}_{k,g}|} \sum_{i \in \mathcal{I}_{k,g}} v_i \leq \epsilon, \quad k \in \mathcal{K} \text{ and } g, g' \in \mathcal{G}. \quad (11)$$

The first term in (10) stands for the fraction of misclassification error made over the samples belonging to the protected group  $g$  for class  $k$ . Likewise, the second term is for the protected group  $g'$ . Due to the absolute value function in (9), we reverse the left-hand side of (10) in (11). Recall that  $v_i$  values in our master problem (3) measure an approximate classification error rather than counting the number of misclassifications. Therefore, (10) and (11) can be considered as soft constraints yielding approximate percentages of unfairness among protected groups and classes in DMC.

When the constraints based on DMC are defined for binary classification and for only two protected groups, that is,  $|\mathcal{K}| = 2$  and  $|\mathcal{G}| = 2$ , (10) and (11) reduce to the fairness definition of *Equalized Odds* used by Lawless et al. (2023). Equalized odds enforces equal false positive rate and false negative rate for both protected groups (see Appendix B). A relaxed version of Equalized Odds is the definition of *Equal Opportunity* that merely mandates an equal false negative rate between two protected groups. This can be achieved by constructing constraints (10) and (11) only for the positive class. Hence, the constraints based on DMC can be used to compute the fairness scores for Equal Opportunity and Equalized Odds. Briefly, the DMC is more general than Equalized Odds, since the terms false positive and false negative in Equalized Odds vanish for multi-class classification.

**Overall Disparate Mistreatment (ODM).** ODM is a generalization of disparate mistreatment (DM) (Zafar et al., 2019), where misclassification rates are equalized in binary classification, to multiple protected groups. Unlike DMC, ODM ignores classes and directly focuses on protected groups to equalize overall misclassification among them. ODM requires that among all protected groups, the overall mistreatment should be the same:

$$P(\hat{y} \neq y | G = g) = P(\hat{y} \neq y | G = g'), \quad g, g' \in \mathcal{G}, \quad (12)$$

where (12) indicates that the probability of incorrect predictions should be equal among protected groups. As in DMC, a certain threshold of  $\epsilon \geq 0$  is used to derive the ODM constraints

$$|P(\hat{y} \neq y | G = g) - P(\hat{y} \neq y | G = g')| \leq \epsilon, \quad g, g' \in \mathcal{G}. \quad (13)$$

Recall that,  $P(\hat{y} \neq y | G = g)$ , describes the total classification error of all samples in the protected group, and the left-hand side of (13) describes the difference of mistreatment between two different protected groups. Let  $\mathcal{I}_g = \{i \in \mathcal{I} : G = g\}$  be the set of samples in protected group  $g$  and  $|\mathcal{I}_g|$  represent its cardinality. Then, we map (13) into the following set of constraints and add them to our LP model (3):

$$\frac{1}{|\mathcal{I}_g|} \sum_{i \in \mathcal{I}_g} v_i - \frac{1}{|\mathcal{I}_{g'}|} \sum_{i \in \mathcal{I}_{g'}} v_i \leq \epsilon, \quad g, g' \in \mathcal{G}, \quad (14)$$

$$\frac{1}{|\mathcal{I}_{g'}|} \sum_{i \in \mathcal{I}_{g'}} v_i - \frac{1}{|\mathcal{I}_g|} \sum_{i \in \mathcal{I}_g} v_i \leq \epsilon, \quad g, g' \in \mathcal{G}. \quad (15)$$

The first and the second terms in (14) stand for the fraction misclassification error made over the samples belonging to the protected groups  $g$  and  $g'$ , respectively. Note that these terms accumulate the error made for all classes  $k \in \mathcal{K}$ .

For the sake of brevity, we skip the details on the derivation of the dual problems and the resulting calculations of the column generation algorithm for the cases when the fairness constraints corresponding to DMC and ODM are added. It is important to note that the

resulting PSP is exactly the same as in (6). Nevertheless, new dual variables are defined for the corresponding constraints (10)–(11) for the DMC, and (14)–(15) for the ODM, respectively, to address fairness. This only affects the dual values of  $\beta$  as the second constraint set in (4) takes a slightly different form without changing the calculation of the reduced cost values in (5). Other aspects of the column generation framework remain the same as before. Besides, the addition of fairness constraints does not affect the feasibility of the dual problem nor requires another initialization scheme of the columns.

**4. Numerical Experiments** We evaluate the performance of the proposed *rule generation algorithm* (RUG) on a collection of standard datasets for classification with the sample sizes ranging from 178 to 245057, the number of classes from 2 to 11, and the number of features from 3 to 166 (see Appendix C for details). We compare our results against three recent algorithms based on mathematical optimization that are the most related ones to our methodology. These are fast sparse decision tree optimization (FSDT) by [McTavish et al. \(2022\)](#), binary optimal classification trees (BinOCT) by [Verwer and Zhang \(2019\)](#), and rule sets via column generation (CG and FairCG for fairness) by [Lawless et al. \(2023\)](#). FSDT and BinOCT are tree-based methods, and CG is a rule-based method. All these approaches consider interpretability. The data must be in binary form for these benchmark methods, specifically FSDT, BinOCT, and CG, and thus, they require pre-processing of the datasets. We use the same binarization scheme as described in the reference study [Lawless et al. \(2023\)](#) for CG, FairCG, FSDT, and BinOCT. To that end, a binary variable is introduced for each category (and for its negation) of a feature. Numerical features are binarized so that the quantiles of the dataset are used as the splitting values and there exists a decile of data between every split. We use ten quantiles for splitting the data as suggested by [Lawless et al. \(2023\)](#). Then, for every split value  $X$ , two binary variables are introduced, one for  $x_p \leq X$  and the other for  $x_p > X$  where  $x_p$  is feature  $p$  with numerical values.

In our experiments, we resort to a five-fold cross-validation scheme combined with grid search for hyperparameter tuning. For FSDT and BinOCT, we select `max_depth` parameter from the set  $\{3,5,10\}$  for maximum tree depth. For RUG, we chose this value from the set  $\{3,5\}$  to generate rules using DTs. Furthermore, for RUG we select the penalty parameter  $\lambda$  (`pen_par`) from the set  $\{0.1,1.0,10.0\}$  and the iteration limit (`max_RMP_calls`) from  $\{5, 10, 15\}$ . We select the rules whose weight  $w_j$  does not exceed 0.05 for prediction. This helps us to reduce the number of rules by discarding the negligible ones. Lastly, we assign the number of features as the cost coefficient of a rule in RUG. For CG, we also perform a grid search for the so-called *complexity parameter*  $C$  defined by [Lawless et al. \(2023\)](#) as an indicator of sparsity. [Lawless et al. \(2023\)](#) report results for mean values of  $C$  per dataset. We cross-validate the complexity parameter  $C$ , considering a set of values around its reported mean value. For example, for a reported mean  $C$  of 25.0, we choose values 20.0, 25.0, and 30.0 for the grid search. The grid search set is limited to three values, all multiples of five, to ensure computational tractability. We impose a running time limit of 300 seconds for all methods. Lastly, all our programs are implemented in Python version 3.10.2 on a computer with an Apple-M1-Pro processor. The resulting LPs and MIP formulations are solved using the Gurobi 10.0.2 solver under its default settings ([Gurobi Optimization, 2023](#)). To reproduce the numerical experiments we refer the reader to our repository\*.

**4.1 Proxy PSP vs. Exact PSP** We compare the efficiency and performance of RUG with the exact PSP formulation (7) against RUG with the proxy PSP on binary classification problems from Appendix C.1. As the exact formulation the PSP requires the data to be in binary form, we apply the process described above to discretize the features. Due to the computational intensity of the exact formulation, the cross-validation scheme with grid search for hyperparameter tuning is nonsensical as it requires an excessively long time. Hence, we apply this process only to the heuristic version of RUG with the proxy PSP, and then run the exact formulation only once with the parameters that worked best for the

\*<https://github.com/sibirbil/RuleDiscovery>

heuristic approach. In Table 9 in Appendix C.2, we report the computation time in seconds in parentheses, the F1-score, and the accuracy. When data is imbalanced, relying only on the accuracy measure can be specious. Therefore, we have also used the F1-score that is less conservative than the accuracy for imbalanced datasets (Japkowicz, 2013). Figure 2 shows the average performance of both approaches over all datasets, *i.e.*, the averaged scores of Table 9.

For each problem, we set a time limit of 300s, after which the current iteration was finished, and then training was stopped and results were inspected. This implies that the number of iterations set by the parameter `max_RMP_calls` may not be reached, and hence, the resulting model has few rules and performance may not be optimal. The heuristic works very fast and training of the model completes within a couple of (milli)seconds, however the exact formulation is computationally quite expensive and almost always hits the imposed time limit. Both the F1-score and accuracy show that the two versions of RUG perform similarly well on most of the datasets. The heuristic shows a slight superiority for most datasets, however it also performs slightly worse on other datasets. On average, the heuristic performs better by about 5% and 1% in terms of F1-score and accuracy, respectively. Hence, it proves to be a good alternative to the exact approach as it reaches very good and similar performance scores within a fraction of the time.

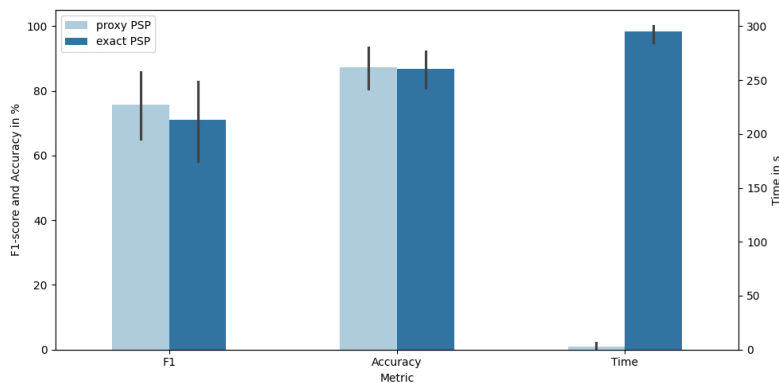


Figure 2: Comparison of metrics between RUG with proxy PSP and RUG with exact PSP.

In the remainder of this section we will compare RUG to other algorithms from the literature. For these comparisons we will rely on the heuristic approach, which we will simply refer to as ‘RUG’.

**4.2 Experiments for Interpretability** We first compare the performance of our algorithm in terms of interpretability against those of FSDT, BinOCT, and CG. Table 1 provides a summary of our results over the binary classification datasets from Appendix C.1. To be specific, each cell in Table 1 is calculated by taking the average of the corresponding columns in Table 10 in Appendix C.3. The first column represents the used method. We report computation time in seconds for each method, along with the F1-score and accuracy as performance indicators under the columns entitled “CPU (s)”, “F1 (%)”, and “Acc. (%)”, respectively. We present the number of rules (“NoR”) and average rule length (“Avg. RL”) in the fifth and the sixth columns to evaluate global interpretability performances. For both tree-based methods FSDT and BinOCT, the number of leaf nodes in their DTs is reckoned as the number of rules. For RUG, the “NoR” corresponds to the number of rules having a weight satisfying the threshold, *e.g.*,  $w_j \geq 0.05$ . For CG, NoR is the number of rules generated by excluding the default rule of assigning an uncovered sample to the majority class from the calculations as this is not generated by the CG. Then, the “Avg. RL” is the average number of levels in the leaf nodes of the DTs for the tree-based methods FSDT and BinOCT, whereas, for RUG (CG), this value is the number of conditions (literals) used in the rules. The last two columns stand for the average number of rules per sample (“Avg.

NoRpS”) and the average rule length per sample (“Avg. RLpS”) as an indicator of local interpretability. The number of rules per sample, “Avg. NoRpS”, gives the number of rules that contribute to classification per sample, *e.g.*, averaged over all samples of the test set. The “Avg. NoRpS” is one for the tree-based methods FSDT and BinOCT, as every sample belongs to a non-overlapping partition of the feature space, resulting in a single rule. In contrast, the rule-based methods RUG and CG can offer multiple rules per sample. This implies that RUG and CG do not offer the same rule (*i.e.*, recipe) for an individual which is advantageous when we prioritize local interpretability. Clearly, there is a trade-off, and the “Avg. NoRpS” should not be excessive as well. RUG strikes a good balance in this respect, offering informative explanations without excessive complexity. The “Avg. RLpS” is similar to the average rule length but takes the average of rule length per sample. Briefly, shorter values of “Avg. RLpS” is considered better for local interpretability.

Table 1: Average results of RUG, FSDT, BinOCT, and CG over binary classification datasets.

	CPU (s)	F1 (%)	Acc. (%)	NoR	Avg.RL	Avg.NoRpS	Avg.RLpS
RUG	3.78	76.96	88.15	42.11	2.96	4.11	3.01
FSDT	163.23	74.14	86.63	18.61	4.27	1.00	3.83
BinOCT	300.00	35.27	371.08	8.00	3.00	1.00	3.00
CG	283.38	68.70	85.59	2.89	4.00	1.21	3.92

The reported results in Table 10 of Appendix C.3 are obtained using the best parameters determined through cross-validation on a hold-out test set that was not used during the training. Overall, RUG outperforms the other methods by more than an order of magnitude in terms of CPU times. RUG also demonstrates superior performance in terms of F1-score and accuracy compared to the other methods. Indeed, RUG achieves an average F1-score of 75.90%, while the closest average F1-score among the other methods is 73.24% by the FSDT. Regarding accuracy, RUG also outperforms the other methods with an average score of 86.91%, followed by 85.29% by FSDT. On the other hand, RUG tends to produce a larger number of rules than the other methods, and the disparity can be substantial for certain instances. However, the “Avg. RL” and the “Avg. RLpS” for RUG are comparable to those of other methods, indicating that RUG achieves enhanced performance while preserving local interpretability. “Avg. NoRpS” for RUG is higher than the other methods. Here, RUG manages to find a fine line for local interpretability by avoiding both excessively high and noticeably low numbers of rules per sample.

We also notice that RUG outperforms the other methods, especially for imbalanced datasets. For example, all methods perform comparably well on MAMOGRAPHY in terms of accuracy, with values ranging from 98.12% (CG) to 98.84% (RUG). However, looking at the F1-score, we observe that, with a score of 70.45%, RUG outperforms the other methods by more than 20%. We can see a similar trend for other datasets, such as MUSK and OILSPILL.

Our comparison with other MOBAs, *i.e.*, FSDT, BinOCT and CG, is limited to binary classification problems as these methods do not address multi-class classification. A common workaround is to apply a *one-vs-rest* scheme, where a classifier for each class is build and the prediction is derived using the predicted probabilities for each class returned by each of the classifiers. Unfortunately this procedure is also not straightforward for the discussed MOBA methods as it requires a predicted probability per class, which these methods do not provide. RUG can directly handle multiple classes without resorting to a *one-versus-rest* scheme. In Table 2, we present results obtained with RUG on a set of multi-class classification problems. We used the same setup for cross-validation and hyperparameter tuning as described above. Although the number of rules reaches to 83.00 for the SENSORLESS dataset, the average rule length, average number of rules per sample, as well as average rule length per sample are relatively small for all datasets. Additionally we report results obtained with traditional machine learning models, specifically decision tree (DT), random forest (RF), AdaBoost (ADA), and light gradient-boosting machine (LightGBM), to judge



RUG’s performance. In general RUG reaches a similar performance in terms of classification accuracy when compared to the other models, in most cases with substantially less rules. For most datasets RUG performs slightly worse than a DT, however with slightly less and also shorter rules, which makes it more interpretable. For the WINE dataset RUG even reaches the same performance as a powerful LightGBM model, with less computation time, shorter and substantially less rules (RUG returns 14 rules, while LightGBM has 1573 rules).

Table 2: Comparison of the performance of RUG and traditional machine learning models on multi-class datasets using five-fold cross validation and grid search for hyperparameter tuning on a hold-out test.

		CPU (s)	weighted F1 (%)	Acc. (%)	NoR	Avg. RL	Avg. NoRps	Avg. RLps
ECOLI	RUG	0.03	75.54	77.94	7.00	2.29	1.29	2.00
	DT	0.01	78.36	79.41	8.00	1.00	3.00	1.00
	RF	0.10	88.16	88.24	5060.00	5.71	150.00	5.61
	ADA	0.07	53.91	66.18	200.00	1.00	100.00	1.00
	LightGBM	1.29	87.30	88.24	14097.00	4.10	2400.00	2.31
GLASS	RUG	0.03	60.57	62.79	17.00	2.47	2.35	2.50
	DT	0.01	63.84	62.79	32.00	5.81	1.0	5.79
	RF	0.07	77.42	76.74	2717.00	5.51	100.00	5.57
	ADA	0.07	24.34	32.56	200.00	1.00	100.00	1.00
	LightGBM	0.65	81.57	81.40	7677.00	3.49	1200.00	3.08
SEEDS	RUG	0.03	90.43	90.48	10.00	2.60	2.40	3.50
	DT	0.01	92.77	92.86	11.00	3.91	1.00	3.31
	RF	0.12	90.43	90.48	2337.00	3.92	200.00	3.37
	ADA	0.06	65.00	71.43	200.00	1.00	100.00	1.00
	LightGBM	0.17	92.77	92.86	1699.00	2.63	300.00	2.73
SENSORLESS	RUG	11.39	79.18	78.42	83.00	4.25	5.33	4.38
	DT	2.06	98.28	98.28	425.00	11.69	1.00	11.42
	RF	17.56	98.44	98.44	56664.00	12.10	100.00	11.06
	ADA	33.30	32.54	45.36	300.00	1.00	150.00	1.00
	LightGBM	42.52	99.97	99.97	48414.00	4.54	3300.00	3.38
WINE	RUG	0.05	97.24	97.22	14.00	1.57	4.39	1.61
	DT	0.01	94.45	94.44	5.00	2.60	1.00	2.44
	RF	0.06	97.24	97.22	639.00	2.74	100.00	2.73
	ADA	0.07	88.49	88.89	200.00	1.00	100.00	1.00
	LightGBM	0.19	97.24	97.22	1573.00	2.51	300.00	2.62

Hyperparameter sets for RUG – max\_depth = {3,5}, pen\_par = {0.1,1.0,10.0}, max\_RMP\_calls = {5,15,30}. Time limit 300s.  
Hyperparameter sets for DT – max\_depth = {3,5,7,9,11,13,15}; for ADA – n\_estimators = {100,150,200,250,300}; for RF and GB – max\_depth = {3,5,7,9,11,13,15}, n\_estimators = {100,150,200,250,300}

**4.3 Experiments for Fairness** We analyze the performance of RUG with fairness constraints, coined as FairRUG, and compare it to FairCG, which is shown to be superior to several state-of-the-art methods by Lawless et al. (2023). As FairCG is designed for binary classification and one sensitive attribute with two groups, our comparison is performed on such datasets. Subsequently, we shall also provide our results for multi-class problems and/or datasets with a sensitive attribute with several groups.

Table 3 presents the results of FairRUG and FairCG that are subject to two fairness constraints concerning *Equal Opportunity* (EOP) and DMC. Observe that FairCG does not address ODM and thus we do not use it for comparison. The first two columns represent the name of the dataset and the method, followed by the computation time in seconds, the F1-score, and the accuracy as before. Columns 6 and 10 provide the fairness scores in percentages under “DMC (%)” and “EOP (%)”. The EOP (see Appendix B for definition) is obtained by relaxing the DMC constraints (10) and (11) for the negative class in FairRUG. The DMC generalizes the fairness definition *Equalized Odds* (EOD) introduced for binary classification. FairCG handles *Equalized Odds* (EOD) which is a special case of DMC. In particular, the DMC and EOD are equivalent to each other and they both measure the difference between false negatives and the difference between false positives of two sensitive attributes in binary classification problems. In short, we simply used DMC for consistency and clarity.

We use five-fold cross-validation for hyperparameter tuning as before. For FairRUG and FairCG, we mostly use the same setup as described for the RUG and CG. However, we set the rule weight threshold of FairRUG to zero and set the rule costs to one since our focus is now on fairness rather than interpretability. Fairness constraints (10), (11), (14) and (15) bring in an additional hyperparameter  $\epsilon$  that needs fine-tuning, which caps the unfairness. Hence, we select  $\epsilon$  from the set  $\{0, 0.01, 0.025, 0.05\}$  for FairRUG. In their study, Lawless et al. (2023) state that the best fairness outcomes are obtained with a cap of  $\epsilon = 0.025$ ,



and thus, we set  $\epsilon = 0.025$  for the FairCG to avoid excessive computational requirements. As usual, we select the hyperparameters in cross-validation, however in this case based on fairness performance rather than accuracy score.

In terms of fairness, we find that FairRUG outperforms FairCG on average. In particular, FairRUG yields the highest fairness scores under DMC constraints for two out of the three datasets. Considering the EOP, FairRUG achieves higher scores for all three datasets. We further see that FairRUG achieves a higher predictive performance, characterized by higher accuracy and F1-scores in all cases except for COMPAS under EOP constraints. Besides, the computation times for FairRUG are significantly better than those of FairCG. In short, FairRUG is capable to strike a favorable balance between fairness and practicality.

Table 3: Accuracy and fairness results of FairRUG and FairCG on binary classification problems.

		CPU (s)	F1 (%)	Acc. (%)	DMC (%)	CPU (s)	F1 (%)	Acc. (%)	EOP (%)
ADULT	FairRUG	32.98	63.81	85.08	89.10	17.37	64.73	85.83	92.39
	FairCG	300.00	11.09	76.86	93.22	300.00	47.66	81.45	64.90
COMPAS	FairRUG	0.04	68.19	68.47	51.89	0.77	63.77	65.62	98.81
	FairCG	300.00	47.73	62.36	17.74	300.00	59.42	66.05	63.93
DEFAULT	FairRUG	9.11	48.27	82.57	97.88	9.10	47.65	82.53	98.69
	FairCG	300.00	41.80	82.08	87.73	300.00	44.82	82.43	89.40

Finally, we compare RUG with FairRUG under fairness constraints using DMC and ODM for the datasets with multi-class targets and/or sensitive attributes with more than two groups in Table 4. We report the computation times in seconds, weighted F1-score, accuracy, and fairness scores for DMC and ODM. Here, the weighted F1-score is calculated using a weighted sum of the F1-scores of each class considering the number of samples from the corresponding class. For RUG no fairness constraints are required and the fairness scores are computed based on the test sample predictions after classification. Therefore, the CPU (s), weighted F1 (%) and Acc. (%) values are the same for both DMC (%) and ODM (%) for RUG. For FairRUG, fairness constraints are added separately for DMC and ODM, and hence, we present values for both models. In general, FairRUG is able to mitigate unfairness in the predictions made by RUG by adding fairness constraints which lead to improved fairness scores. This is expected especially when there exists a bias against a protected group in the dataset. However, RUG also shows a very high performance that equals that of FairRUG in case of both the NURSERY and LAW datasets. First, a lack of bias in a dataset can positively impact machine learning methods that are equity-unaware but accurate like RUG. Second, incorporating fairness constraints may not yield equivalent benefits on the test samples due to learning being performed on the training set. We observe this property for the fairness scores on the STUDENT dataset, where fairness slightly deteriorates for FairRUG.

Table 4: Accuracy and fairness results of RUG and FairRUG.

		CPU (s)	weighted F1 (%)	Acc. (%)	DMC (%)	CPU (s)	weighted F1 (%)	Acc. (%)	ODM (%)
ATTRITION	RUG	0.15	30.51	86.05	97.46	-	-	-	72.04
	FairRUG	0.23	25.45	86.05	93.58	0.48	34.78	84.69	78.87
NURSERY	RUG	0.75	100.00	100.00	100.00	-	-	-	100.00
	FairRUG	1.11	100.00	100.00	100.00	1.00	100.00	100.00	100.00
STUDENT	RUG	0.08	75.04	75.38	89.22	-	-	-	88.26
	FairRUG	0.29	61.15	60.77	81.54	0.13	70.31	70.77	84.96
LAW	RUG	0.44	100.00	100.00	100.00	-	-	-	100.00
	FairRUG	0.69	100.00	100.00	100.00	4.32	100.00	100.00	100.00

ATTRITION is a binary classification problem with a sensitive attribute with more than two groups. NURSERY, STUDENT, and LAW are multiclass problems.

**4.4 Case Study: Credit Risk Scoring** In this case study, we look at credit risk modeling in the banking industry. The LOAN dataset (available on Kaggle) holds information on consumer loans issued by the Lending Club, a peer-to-peer lender. The raw dataset holds data on over 450,000 consumer loans issued between 2007 and 2014 with 73 features and one target variable. After pre-processing, the final dataset consists of 395,492 samples with 42 features, including one-hot encoded features for categorical variables. The target variable is binary and indicates good or bad credit risk. Since the distribution of the target variable is highly imbalanced, with only 10% of instances belonging to the positive class, we focus on both accuracy and F1-score as performance indicators. We look at the average rule length (Avg.RL), the number of rules (NoR), the average rule length per sample (Avg.RLpS), and the average number of rules per sample (Avg.NoRpS) as before.

For consistency, we first focus on interpretability only and compare the results of RUG with results obtained with FSDT (McTavish et al., 2022), CG (Lawless et al., 2023) and BinOCT (Verwer and Zhang, 2019). Since shorter rules are considered to be more interpretable, we set the parameter for the maximum tree depth to two for FSDT, BinOCT and RUG. For RUG, we set the cost coefficients  $c_j$ 's to be equal to the rule length, *i.e.*, number of conditions in the rule. Our results are reported in Table 5. RUG generates only seven rules, with which we can reach an accuracy of 97.55% and an F1-score of 87.50%. On average, 1.25 rules are used per sample to predict the target. With `max_depth` set to two, the average rule length as well as the average rule length per sample is also equal to two. FSDT, with four rules, achieves a relatively good accuracy of 95.72% with an F1-score of only 81.41%. BinOCT performs quite poorly with a F1-score of 0.00 and an accuracy of 89.95%. The complexity hyperparameter  $C$  of CG needed to be set to five for it to return at least one rule. CG shows worse performance than both FSDT and RUG with an accuracy of 92.24% and a much lower F1-score of only 39.47%.

Table 5: Interpretability case study results obtained with different methods when the focus is on interpretability.

	<b>F1 (%)</b>	<b>Acc. (%)</b>	<b>NoR</b>	<b>Avg.RL</b>	<b>Avg.NoRpS</b>	<b>Avg.RLpS</b>
RUG	87.50	97.55	7.00	2.00	1.25	2.00
FSDT	81.41	95.72	4.00	2.00	1.00	2.00
BinOCT	0.00	89.95	4.00	2.00	1.00	2.00
CG	39.47	92.24	1.00	4.00	1.00	4.00

Avg.RL: Average rule length; NoR: Number of rules; Avg.NoRpS: Average number of rules per sample; Avg.RLpS: Average rule length per sample

Table 6: Interpretability case study results obtained with different methods when the focus is on accuracy.

	<b>F1 (%)</b>	<b>Acc. (%)</b>	<b>NoR</b>	<b>Avg.RL</b>	<b>Avg.NoRpS</b>	<b>Avg.RLpS</b>
RUG	94.68	98.96	44.00	1.98	6.55	2.00
FSDT	85.56	97.23	8.00	3.00	1.00	3.00
BinOCT	–	–	–	–	–	–
CG	59.05	93.89	4.00	4.50	1.35	4.95

Avg.RL: Average rule length; NoR: Number of rules; Avg.NoRpS: Average number of rules per sample; Avg.RLpS: Average rule length per sample

Next, we try to boost the performance of all methods by relaxing some parameters, while still keeping the models interpretable. To that end, we allow higher `max_depth` values for the trees of the FSDT, and the complexity parameter  $C$  of the CG as well as the number of iterations in RUG. For the FSDT, the best value for the depth of the trees was three; for the CG the best value for the complexity parameter was 25. BinOCT struggled with a higher depth parameter and a dataset of this size, and execution failed. This may of course also be due to limitations imposed by the hardware used to run these experiments. We report these results in Table 6. RUG returns 44 rules with an average length of 1.98. The accuracy reaches 98.96% and the F1-score increases to 94.68% while maintaining a good level of local interpretability with an average of 6.55 rules per sample. Both CG and FSDT have better global interpretability considering their fewer rules, however, their accuracy does not match that of RUG and the F1-scores are lower with 85.56% for the FSDT and 59.05% for the CG.

To evaluate the performance of RUG further, we also apply SHAP (Lundberg and Lee, 2017) to LightGBM that we train on the dataset and compare its output to that of RUG (from Table 5). With 80 rules, an average rule length of 2, and 20 rules on average per sample, the trained LightGBM model has a F1-score of 87.06% and an accuracy of 97.27%. SHAP produces local explanations per sample in terms of feature weights and associates feature importance plots. Typically, in a feature importance plot, the features are sorted

in descending order of the magnitudes of their weights, and the signs of the weights are depicted with two different colors. We have compared the SHAP output against the rules and the associated features obtained by RUG. In Figure 3, we display the SHAP plots for two rejected samples (class 0) alongside the rules generated by RUG that cover those samples. The first sample (Figure 3 left) is covered by two rules, rule 1 and rule 6, which use features called as `last_pymnt_amnt`, `mths_since_issue_d`, and `mths_since_last_pymnt_d`. These features are also among the four most important according to SHAP. The second sample (Figure 3 right) is covered by just one rule, rule 3. Similarly, the features utilized by this rule belong to the features with the highest three contributing to the prediction of the LightGBM model. This exemplifies the advantage of using RUG for local explanations as an in-processing method. Indeed, RUG does not need an additional explanation step such as SHAP, being a post-processing method which requires substantial computational effort to yield an output.

In Appendix D, we present further results on the case study where we compare RUG to traditional machine learning models including Logistic Regression (LR), Decision Tree (DT), Random Forest (RF), AdaBoost (ADA) (Freund and Schapire, 1997), and LightGBM (Ke et al., 2017). Besides, we introduce an implementation of RUG in practice at a consultancy firm.

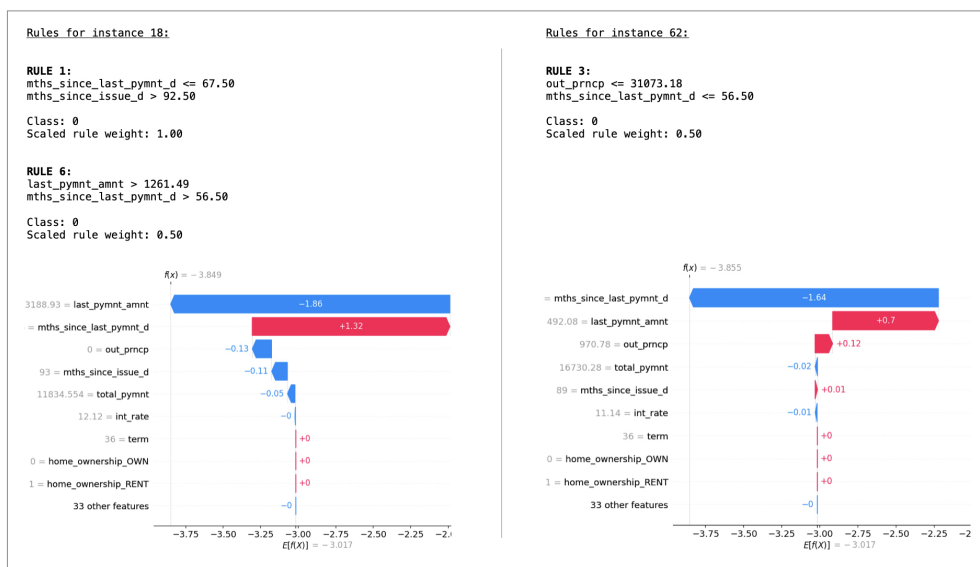


Figure 3: Local interpretations for two samples (left and right). The rules used by RUG to classify the samples are given above the feature importance plots that are produced after applying SHAP to the trained LightGBM model.

**5. Conclusion** We have proposed a Linear Programming (LP) based rule generation framework to discover a set of rules for multi-class classification problems. The proposed LP-based framework is more advantageous than existing mathematical optimization-based approaches (MOBAs) that use mixed-integer linear programming (MILP) due to its scalability for large datasets. Our methodology is flexible to address interpretability and fairness both of which are salient to support the trustworthiness of algorithms in automated decision making.

The objective of our LP formulation is to find a set of rules and their associated weights such that the sum of the classification error and the total rule cost is minimized. The rule costs can promote shorter rules in the LP model for better interpretability. Optimal rule weights from the LP model facilitate interpretation for classification by attaching importance to the rules.

Fairness often arises in the form of constraints to eliminate discrimination among protected and unprotected social groups in society. Most of the fairness definitions are designed for binary classification problems. We introduce two fairness notions that address multiple classes and multiple sensitive attributes (protected groups) for group fairness.

We solve our LP using column generation. A significant advantage of this is having more control over the generation of the rules. We argue that it is still challenging to optimally solve the pricing subproblem as we have shown it to be NP-hard. As a remedy, we have proposed to solve a proxy subproblem by training decision trees with sample weights. These sample weights are obtained from the dual of the linear programs. In fact, training decision trees with sample weights are very fast, and also standard in most machine-learning packages. Such a column generation approach combined with solving the pricing subproblem quickly brings further scalability.

We have demonstrated the performance of the proposed methodology using standard test instances from the literature as well as a case study. The numerical experiments have shown that our framework can be used to compromise the balance among accuracy, interpretability, and fairness. The case study is concerned with credit risk scoring in the banking industry and addresses interpretability.

We observe that our rule generation algorithm, RUG is highly scalable for large datasets unlike other MOBAs considered. RUG outperforms other methods in terms of both accuracy and F1-scores. Benchmark MOBAs perform very well for global interpretability. Nevertheless, RUG focuses on local interpretability with an aim to provide individual explanations for which those benchmark studies struggle since every individual is mostly treated using the same few rules.

This study is conducted for multi-class classification. As further research, our linear programming model can be reformulated for regression problems using a piecewise-linear loss function (*e.g.*, mean absolute deviation). This requires analyzing the resulting pricing subproblems and the usage of new heuristic approaches if possible. Last but not least, robustness of the generated rules can be considered as a fruitful future research direction.

**Acknowledgement** The authors are thankful to Emre Can Yayla for his help with the preparation of datasets.

## References

- Aghaei, S., Gómez, A., and Vayanos, P. (2021). Strong optimal classification trees. *arXiv preprint*. <https://arxiv.org/pdf/2103.15965.pdf>.
- Alghamdi, W., Hsu, H., Jeong, H., Wang, H., Michalak, P. W., Asoodeh, S., and Calmon, F. P. (2022). Beyond adult and compas: Fairness in multi-class prediction. *arXiv preprint*. <https://arxiv.org/pdf/2206.07801.pdf>.
- Alston, B., Validi, H., and Hicks, I. V. (2022). Mixed integer linear optimization formulations for learning optimal binary classification trees. *arXiv preprint*. <https://arxiv.org/pdf/2206.04857.pdf>.
- Arrieta, A. B., Díaz-Rodríguez, N., Del Ser, J., Bennetot, A., Tabik, S., Barbado, A., García, S., Gil-López, S., Molina, D., Benjamins, R., et al. (2020). Explainable artificial intelligence (XAI): Concepts, taxonomies, opportunities and challenges toward responsible AI. *Information Fusion*, 58:82–115.
- Barocas, S., Hardt, M., and Narayanan, A. (2023). *Fairness and Machine Learning: Limitations and Opportunities*. MIT Press. <http://www.fairmlbook.org>.
- Berk, R., Heidari, H., Jabbari, S., Kearns, M., and Roth, A. (2021). Fairness in criminal justice risk assessments: The state of the art. *Sociological Methods & Research*, 50(1):3–44.

- Bertsimas, D., Delarue, A., Jaillet, P., and Martin, S. (2019). The price of interpretability. arXiv preprint. <https://arxiv.org/pdf/1907.03419.pdf>.
- Bertsimas, D. and Dunn, J. (2017). Optimal classification trees. *Machine Learning*, 106(7):1039–1082.
- Blanquero, R., Carrizosa, E., Molero-Río, C., and Morales, D. R. (2019). Sparsity in optimal randomized classification trees. *European Journal of Operational Research*, 284(1):255–272.
- Carrizosa, E., Molero-Río, C., and Romero Morales, D. (2021). Mathematical optimization in classification and regression trees. *TOP*, 29(1):5–33.
- Chouldechova, A. (2017). Fair prediction with disparate impact: A study of bias in recidivism prediction instruments. *Big Data*, 5(2):153–163.
- Church, R. and ReVelle, C. (1974). The maximal covering location problem. In *Papers of the Regional Science Association*, volume 32, pages 101–118. Springer-Verlag Berlin/Heidelberg.
- Dash, S., Günlük, O., and Wei, D. (2018). Boolean decision rules via column generation. In Bengio, S., Wallach, H., Larochelle, H., Grauman, K., Cesa-Bianchi, N., and Garnett, R., editors, *Advances in Neural Information Processing Systems*, volume 31, pages 1–11. Curran Associates, Inc.
- Demiriz, A., Bennett, K. P., and Shawe-Taylor, J. (2002). Linear programming boosting via column generation. *Machine Learning*, 46(1-3):225–254.
- Demirović, E., Lukina, A., Hebrard, E., Chan, J., Bailey, J., Leckie, C., Ramamohanarao, K., and Stuckey, P. J. (2022). MurTree: Optimal decision trees via dynamic programming and search. *Journal of Machine Learning Research*, 23(26):1–47.
- Denis, C., Elie, R., Hebiri, M., and Hu, F. (2021). Fairness guarantee in multi-class classification. arXiv preprint. <https://arxiv.org/pdf/2109.13642.pdf>.
- Desaulniers, G., Desrosiers, J., and Solomon, M. M. (2006). *Column Generation*, volume 5. Springer Science & Business Media.
- Downs, B. T. (1991). *A robust dual-based solution algorithm for the maximal covering problem*. Unpublished doctoral dissertation, University of Cincinnati.
- Dua, D. and Graff, C. (2017). UCI machine learning repository.
- Dwork, C., Hardt, M., Pitassi, T., Reingold, O., and Zemel, R. (2012). Fairness through awareness. In *Proceedings of the 3rd Innovations in Theoretical Computer Science Conference, ITCS '12*, page 214–226, New York, NY, USA. Association for Computing Machinery. <https://doi.org/10.1145/2090236.2090255>.
- Firat, M., Crognier, G., Gabor, A. F., Hurkens, C. A., and Zhang, Y. (2020). Column generation based heuristic for learning classification trees. *Computers & Operations Research*, 116:104866.
- Freund, Y. and Schapire, R. E. (1997). A decision-theoretic generalization of on-line learning and an application to boosting. *Journal of Computer and System Sciences*, 55(1):119–139.
- Fürnkranz, J. (1999). Separate-and-conquer rule learning. *Artificial Intelligence Review*, 13(1):3–54.
- Gambella, C., Ghaddar, B., and Naoum-Sawaya, J. (2021). Optimization problems for machine learning: A survey. *European Journal of Operational Research*, 290(3):807–828.

- Gehler, P. and Nowozin, S. (2009). On feature combination for multiclass object classification. In 2009 IEEE 12th International Conference on Computer Vision, pages 221–228. IEEE Xplore.
- Ghosh, B. and Meel, K. S. (2019). Imli: An incremental framework for maxsat-based learning of interpretable classification rules. In Proceedings of the 2019 AAAI/ACM Conference on AI, Ethics, and Society, AIES '19, page 203–210, New York, NY, USA. Association for Computing Machinery.
- Guidotti, R., Monreale, A., Ruggieri, S., Pedreschi, D., Turini, F., and Giannotti, F. (2018). Local rule-based explanations of black box decision systems. arXiv preprint. <https://arxiv.org/pdf/1805.10820.pdf>.
- Günlük, O., Kalagnanam, J., Li, M., Menickelly, M., and Scheinberg, K. (2021). Optimal decision trees for categorical data via integer programming. Journal of Global Optimization, 81(1):233–260.
- Gurobi Optimization, L. (2023). Gurobi optimizer reference manual. <https://www.gurobi.com>.
- Hardt, M., Price, E., Price, E., and Srebro, N. (2016). Equality of opportunity in supervised learning. In Lee, D., Sugiyama, M., Luxburg, U., Guyon, I., and Garnett, R., editors, Advances in Neural Information Processing Systems, volume 29. Curran Associates, Inc.
- Hastie, T., Tibshirani, R., Friedman, J. H., and Friedman, J. H. (2009). The Elements of Statistical Learning: Data Mining, Inference, and Prediction, volume 2. Springer.
- Ignatiev, A., Marques-Silva, J., Narodytska, N., and Stuckey, P. J. (2021). Reasoning-based learning of interpretable ML models. In 30th International Joint Conference on Artificial Intelligence (IJCAI 2021), pages 4458–4465.
- Japkowicz, N. (2013). Assessment Metrics for Imbalanced Learning, chapter 8, pages 187–206. John Wiley & Sons, Ltd.
- Jo, N., Aghaei, S., Benson, J., Gómez, A., and Vayanos, P. (2022). Learning optimal fair classification trees. arXiv preprint. <https://arxiv.org/pdf/2201.09932.pdf>.
- Ke, G., Meng, Q., Finley, T., Wang, T., Chen, W., Ma, W., Ye, Q., and Liu, T.-Y. (2017). Lightgbm: A highly efficient gradient boosting decision tree. In Guyon, I., Luxburg, U. V., Bengio, S., Wallach, H., Fergus, R., Vishwanathan, S., and Garnett, R., editors, Advances in Neural Information Processing Systems, volume 30. Curran Associates, Inc.
- Kearns, M., Li, M., and Valiant, L. (1994). Learning boolean formulas. Journal of the ACM (JACM), 41(6):1298–1328.
- Kubat, M., Holte, R. C., and Matwin, S. (1998). Machine learning for the detection of oil spills in satellite radar images. Machine Learning, 30(2):195–215.
- Lakkaraju, H., Bach, S. H., and Leskovec, J. (2016). Interpretable decision sets: A joint framework for description and prediction. In Proceedings of the 22nd ACM SIGKDD International Conference on Knowledge Discovery and Data Mining, KDD '16, page 1675–1684, New York, NY, USA. Association for Computing Machinery.
- Lawless, C., Dash, S., Günlük, O., and Wei, D. (2023). Interpretable and fair boolean rule sets via column generation. Journal of Machine Learning Research, 24(229):1–50.
- Liu, Y. (2022). bsnsing: A decision tree induction method based on recursive optimal boolean rule composition. INFORMS Journal on Computing, 34(6):2908–2929.



- Lundberg, S. M. and Lee, S.-I. (2017). A unified approach to interpreting model predictions. In Guyon, I., Luxburg, U. V., Bengio, S., Wallach, H., Fergus, R., Vishwanathan, S., and Garnett, R., editors, Advances in Neural Information Processing Systems, volume 30. Curran Associates, Inc.
- Malioutov, D. and Meel, K. S. (2018). MLIC: A maxsat-based framework for learning interpretable classification rules. In Hooker, J., editor, Principles and Practice of Constraint Programming, pages 312–327, Cham. Springer International Publishing.
- Malioutov, D. and Varshney, K. (2013). Exact rule learning via boolean compressed sensing. In Dasgupta, S. and McAllester, D., editors, Proceedings of the 30th International Conference on Machine Learning, volume 28 of Proceedings of Machine Learning Research, pages 765–773, Atlanta, Georgia, USA. PMLR.
- McTavish, H., Zhong, C., Achermann, R., Karimalis, I., Chen, J., Rudin, C., and Seltzer, M. (2022). Fast sparse decision tree optimization via reference ensembles. In Proceedings of the AAAI Conference on Artificial Intelligence, volume 36, pages 9604–9613. PKP Publishing Services.
- Molnar, C. (2022). Interpretable Machine Learning. A Guide for Making Black Box Models Explainable. <https://christophm.github.io/interpretable-ml-book/>, 2<sup>nd</sup> edition.
- Proença, H. M. and van Leeuwen, M. (2020). Interpretable multiclass classification by MDL-based rule lists. Information Sciences, 512:1372–1393.
- Rivest, R. L. (1987). Learning decision lists. Machine learning, 2:229–246.
- Saffari, A., Godec, M., Pock, T., Leistner, C., and Bischof, H. (2010). Online multi-class LPBoost. In 2010 IEEE Computer Society Conference on Computer Vision and Pattern Recognition, pages 3570–3577. IEEE Xplore.
- Verwer, S. and Zhang, Y. (2019). Learning optimal classification trees using a binary linear program formulation. In Proceedings of the AAAI Conference on Artificial Intelligence, volume 33, pages 1625–1632. PKP Publishing Services.
- Wan, M., Zha, D., Liu, N., and Zou, N. (2023). In-processing modeling techniques for machine learning fairness: A survey. ACM Transactions on Knowledge Discovery from Data, 17(3):1–27.
- Wang, T. and Rudin, C. (2015). Learning optimized Or’s of And’s. arXiv preprint. <https://arxiv.org/pdf/1511.02210.pdf>.
- Wang, T., Rudin, C., Doshi-Velez, F., Liu, Y., Klampff, E., and MacNeille, P. (2017). A Bayesian framework for learning rule sets for interpretable classification. The Journal of Machine Learning Research, 18(1):2357–2393.
- Wang, Y., Wang, D., Geng, N., Wang, Y., Yin, Y., and Jin, Y. (2019). Stacking-based ensemble learning of decision trees for interpretable prostate cancer detection. Applied Soft Computing, 77:188–204.
- Wei, D., Dash, S., Gao, T., and Günlük, O. (2019). Generalized linear rule models. arXiv preprint. <https://arxiv.org/pdf/1906.01761.pdf>.
- Yang, L. and van Leeuwen, M. (2022). Truly unordered probabilistic rule sets for multi-class classification. arXiv preprint. <https://arxiv.org/pdf/2206.08804.pdf>.
- Zafar, M. B., Valera, I., Gomez-Rodriguez, M., and Gummadi, K. P. (2019). Fairness constraints: A flexible approach for fair classification. The Journal of Machine Learning Research, 20(1):2737–2778.
- Zhu, J., Zou, H., Rosset, S., and Hastie, T. (2009). Multi-class Adaboost. Statistics and Its Interface, 2(3):349–360.

## Appendices

**Appendix A. Proof of Proposition 3.2** We show that the “*decision version of the PSP*” (“*d-PSP*” for short) represented with (7) is NP-complete by reduction from Maximal Coverage Location Problem (MCLP) presented in Church and ReVelle (1974). The proof consists of three parts: *i*) reformulation of the d-PSP represented with (7) as an equivalent mathematical program that can be done in polynomial time, *ii*) introduction of the MCLP formulation that reduces to an instance of the d-PSP, and *iii*) transformation of their solutions to each other. In what follows, we present these three parts in detail.

*i*) We state the decision problem as follows. “Is there a negative reduced cost rule with  $c$  features?” Clearly, there can be at most  $|\mathcal{P}|$  features selected in a rule and the optimum can be found in polynomial time of the number of features by solving for  $c = 1, \dots, |\mathcal{P}|$  and choosing the minimum reduced cost rule among them. Therefore, if one can solve the d-PSP in polynomial time, then the PSP can also be solved in polynomial time by solving the d-PSP  $|\mathcal{P}|$  times ( $|\mathcal{P}|$  is polynomial in the length of the input, e.g. number of features).

We derive an equivalent formulation for the d-PSP. To that end, we add the following constraint  $\sum_{p \in \mathcal{P}} (1 - s_p) = c$  into the formulation. Moreover, it is possible to simplify (7) by reversing the definition of variables using variable transformation. Let’s substitute  $1 - s_p$  with a new binary variable  $z_p$  that becomes one if and only if feature  $p$  is not selected in the rule and zero otherwise. Similarly, we substitute  $1 - a_i$  with the binary variable  $b_i$  which is equal to 1 when the sample is not covered by the rule, and zero otherwise. All these operations can be done with  $|\mathcal{P}| + |\mathcal{I}|$  substitutions. Let  $\mathcal{P}_i$  denote the set of features needed in the rule to cover sample  $i$ , e.g.  $\mathcal{P}_i = \{p \in \mathcal{P} : x_{ip} = 1\}$ . Then, the d-PSP is formulated as follows:

$$\begin{aligned}
& \text{maximize} && \sum_{i \in \mathcal{I}^-} b_i \beta_i - \sum_{i \in \mathcal{I}^+} b_i \beta_i + C \\
& \text{subject to} && \sum_{p \in \mathcal{P}_i} z_p \geq b_i && i \in \mathcal{I}, \\
& && z_p \leq b_i && i \in \mathcal{I}, p \in \mathcal{P}_i, \\
& && \sum_{p \in \mathcal{P}} z_p = c, && \\
& && b_i \in \{0, 1\} && i \in \mathcal{I}, \\
& && z_p \in \{0, 1\} && p \in \mathcal{P}.
\end{aligned} \tag{16}$$

The constant term represented with  $C$  is as follows  $C = \sum_{i \in \mathcal{I}^+} \beta_i - \sum_{i \in \mathcal{I}^-} \beta_i - \lambda c$  and should be added to the objective in (16) yet this does not affect the optimal solution. Besides, we can replace the second constraint set in (16) with

$$\frac{1}{|\mathcal{P}_i|} \sum_{p \in \mathcal{P}_i} z_p \leq b_i \quad i \in \mathcal{I}. \tag{17}$$

Constraints (17) can be obtained by summing over the second constraints of (16) for  $p \in \mathcal{P}_i$ . Lastly, the decision version of the PSP represented with (7) is equivalently represented as follows:

$$\begin{aligned}
& \text{maximize} && \sum_{i \in \mathcal{I}^-} b_i \beta_i - \sum_{i \in \mathcal{I}^+} b_i \beta_i + C \\
& \text{subject to} && \sum_{p \in \mathcal{P}_i} z_p \geq b_i && i \in \mathcal{I}, \\
& && \frac{1}{|\mathcal{P}_i|} \sum_{p \in \mathcal{P}_i} z_p \leq b_i && i \in \mathcal{I}, \\
& && \sum_{p \in \mathcal{P}} z_p = c, && \\
& && b_i \in \{0, 1\} && i \in \mathcal{I}, \\
& && z_p \in \{0, 1\} && p \in \mathcal{P}.
\end{aligned} \tag{18}$$

*ii*) Now, we introduce the MCLP formulation (Church and ReVelle, 1974) that is used

for reduction:

$$\max \left\{ \sum_{h \in \mathcal{H}} A_h Y_h : \sum_{l \in \mathcal{L}_h} X_l \geq Y_h, h \in \mathcal{H}; \sum_{l \in \mathcal{L}} X_l = T; X \in \{0, 1\}^{|\mathcal{L}|}, Y \in \{0, 1\}^{|\mathcal{H}|} \right\}. \quad (19)$$

The objective of the MCLP is to maximize the weighted number of  $h \in \mathcal{H}$  demand nodes having weight of  $A_h \geq 0$  where  $Y_h$  denotes the binary variable showing whether demand node  $h$  is covered or not.  $\mathcal{L}$  is the set of facility nodes and  $X_l$  stands for the binary variable to open facility  $l \in \mathcal{L}$ .  $T$  is the number of facility nodes to open given in the second constraint as  $\sum_{l \in \mathcal{L}} X_l = T$ .  $\mathcal{L}_h$  is the set of facility nodes that can serve demand node  $h$ , and, thus, the first constraints are coverage constraints for each demand node  $h$ .

We solve a d-PSP instance with  $\beta_i = 0$  for  $i \in \mathcal{I}^+$  and for each  $i \in \mathcal{I}$  define a demand node  $h$  with  $A_h = \beta_i$ . Define for each feature  $p \in \mathcal{P}$  a facility node  $l$  and let  $\mathcal{P}_i$  be the set of demand nodes  $h$  that can be served by facility node  $l \in \mathcal{L}_h$ . Also, set  $c = T$  as the number of facility nodes to open.

*iii)* Lastly, we show how to transform solutions of the d-PSP and the MCLP to each other. Given an optimal solution  $(\mathbf{b}^*, \mathbf{z}^*)$  of the d-PSP instance,  $(\mathbf{b}^*, \mathbf{z}^*)$  is also optimal for the MCLP. Observe that, by selection of  $\beta_i \geq 0$  values constraints  $\frac{1}{|\mathcal{P}_i|} \sum_{p \in \mathcal{P}_i} z_p \leq b_i$  are redundant for  $i \in \mathcal{I}^-$  since a sample  $i \in \mathcal{I}^-$  is enforced to one as long as  $\sum_{p \in \mathcal{P}_i} z_p > 0$ . Besides, samples  $i \in \mathcal{I}^+$  has no effect on the objective as  $\beta_i = 0$  which renders both of the following constraints  $\sum_{p \in \mathcal{P}_i} z_p \geq b_i$  and  $\frac{1}{|\mathcal{P}_i|} \sum_{p \in \mathcal{P}_i} z_p \leq b_i$  redundant for  $i \in \mathcal{I}^+$ . Thus,  $(\mathbf{b}^*, \mathbf{z}^*)$  is also optimal for the MCLP. Assume that  $(\mathbf{b}^*, \mathbf{z}^*)$  is not optimal for the MCLP, then there exists a solution  $(\bar{\mathbf{b}}^*, \bar{\mathbf{z}}^*)$  with a better objective. We can set  $b_i = \bar{b}_i^*$  for  $i \in \mathcal{I}^-$ . For each sample  $i \in \mathcal{I}^+$ , we can check in polynomial time to find binding constraints in (18). We can set  $b_i = 0$  when  $\sum_{p \in \mathcal{P}_i} z_p = 0$  and  $b_i = 1$  otherwise without changing the objective value of the d-PSP. This implies that we can find a better objective than  $(\mathbf{b}^*, \mathbf{z}^*)$  which is a contradiction. This implies that the d-PSP is NP-complete by reduction from the MCLP which is NP-hard as shown by Downs (1991). Consequently, the PSP represented with (7) is also NP-hard.

**Appendix B. Fairness Discussion** In this section, we discuss relevant fairness notions from the literature for both binary and multi-class classification. Our fairness definitions introduced in section 3.4 build upon this prior work.

**Binary Classification.** Let  $y \in \{+1, -1\}$  stand for the labels of the samples having a positive (+1) or negative label (-1), and  $\hat{y} \in \{+1, -1\}$  is the prediction of a classifier. Then, the total numbers of samples are represented as True Positive (TP) when  $y = \hat{y} = +1$ , as False Positive (FP) when  $y = -1, \hat{y} = +1$ , as False Negative (FN) when  $y = +1, \hat{y} = -1$ , and as True Negative (TN) when  $y = \hat{y} = -1$ . These numbers are then used by performance measures of binary classifiers.

Let  $\mathcal{G}$  be the set of protected groups  $g \in \mathcal{G}$  having distinct sensitive characteristics. Consider  $g \in \mathcal{G} \equiv \{0, 1\}$  showing that there are two protected groups, for instance, based on gender, where  $g = 1$  and  $g = 0$  represent female and male individuals, respectively. The fairness notions are established using empirical probabilities, which are then transformed into fairness constraints. [Hardt et al. \(2016\)](#) define *Equalized Odds* (EOD) and its relaxation *Equal Opportunity* (EOP) for binary classification as follows:

$$\text{Equalized Odds: } P(\hat{y} = +1|y = a, g = 1) = P(\hat{y} = +1|y = a, g = 0), \quad a \in \{+1, -1\}, \quad (20)$$

$$\text{Equal Opportunity: } P(\hat{y} = +1|y = +1, g = 1) = P(\hat{y} = +1|y = +1, g = 0). \quad (21)$$

These equalities indicate that the probability of predicting a positive class should be equal for both protected groups. EOD considers both TP and FP, whereas EOP addresses only TP. In fact, [Lawless et al. \(2023\)](#) define EOP and EOD differently such that EOD takes into account FP and FN while EOP seeks for equality of FN among protected groups. When we swap the labels of samples with each other in [Lawless et al. \(2023\)](#), the EOP concept becomes identical in both studies ([Hardt et al., 2016](#); [Lawless et al., 2023](#)). Unfortunately, a similar conclusion does not hold for the fairness notion using EOD. Akin to EOD by [Lawless et al. \(2023\)](#), *error rate balance* (ERB) is used as the fairness notion by [Chouldechova \(2017\)](#) to equalize both error rates FP and FN among protected groups. Recently, [Berk et al. \(2021\)](#) name ERB as *conditional procedure error* and overall error as *overall procedure error* (OPE). To sum up, there is an abundance of fairness notions even for the binary classification, and consequently, it is fair to say that fairness terminology is not settled yet. Here, we concentrate on *separation* criterion which implies that given a class of observations, the prediction is independent of the sensitive attribute as defined in [Barocas et al. \(2023\)](#). This reduces to equality of error rates among protected groups.

**Multi-Class Classification.** Fairness definitions start to levitate in a multi-class setting. The metrics TP, FP, TN, and FN require a positive and a negative class. Then, the consideration of other classes follows and multi-class setting eviscerates the meaning of TP, FP, FN, and TN. [Denis et al. \(2021\)](#) generalize *demographic parity* (DP) definition into multi-class such that DP imposes equal prediction probability of each class among the protected groups. DP is being criticized by [Dwork et al. \(2012\)](#) that it might yield unfair outcomes for individuals while trying to guarantee equality among protected groups. [Alghamdi et al. \(2022\)](#) modify DP, EOD, and *overall accuracy equality* (OAE) into a multi-class multiple protected groups setting by post-processing whereas our methodology belongs to in-processing techniques (see [Wan et al., 2023](#)). Observe that, maximizing overall accuracy corresponds to minimizing overall error. In that sense, they can be considered as complementing each other. [Zafar et al. \(2019\)](#) use the term *disparate mistreatment* (DM) where misclassification rate among protected groups are equalized for binary classification. We also denominate our fairness notions using a similar terminology with [Zafar et al. \(2019\)](#) and choose DM in our definitions.

**Appendix C. Numerical Experiments** In this section we provide more detail on the datasets used for our numerical experiments. We also extend the case study from 4.4 by comparing the performance of our algorithm to traditional machine learning models.

### C.1 Dataset properties

Table 7: Properties of the datasets used for the numerical experiments on interpretability.

	Sample Size	Classes	Features	Encoded features	Binarized features	Imbalance (%)
ADULT	32561	2	14	107	262	24.08
BANK-MKT	11162	2	16	51	180	47.38
BANKNOTE	1372	2	4	4	72	44.46
DIABETES	768	2	8	8	134	34.90
HEARTS	303	2	13	27	128	54.46
ILPD	583	2	10	10	158	28.50
IONOSPHERE	351	2	34	34	566	64.10
LIVER	345	2	6	6	104	57.97
LOAN	395492	2	21	42	302	10.05
MAGIC	19020	2	10	10	180	64.84
MAMMOGRAPHY	11183	2	6	6	70	2.32
MUSHROOM	8124	2	22	117	234	51.80
MUSK	6598	2	166	166	2922	15.41
OILSPILL	937	2	49	48	772	4.38
PHONEME	5404	2	5	5	90	29.35
SKINNONSKIN	245057	2	3	3	54	79.25
TIC-TAC-TOE	958	2	9	27	54	65.34
TRANSFUSION	748	2	4	4	64	23.80
WDBC	569	2	30	30	540	37.26
ECOLI	336	8	7	7	94	—
GLASS	214	6	9	9	138	—
SEEDS	210	3	7	7	126	—
SENSORLESS	58509	11	48	48	864	—
WINE	178	3	13	13	234	—

PHONEME is from an online repository: <https://datahub.io/machine-learning/phoneme>; OILSPILL comes from Kubat et al. (1998); All remaining datasets come from Dua and Graff (2017)

Table 8: Properties of the datasets used for the numerical experiments for fairness.

	Sample Size	Classes	Features	Encoded features	Binarized features	Sensitive attribute	Groups
ADULT	32561	2	14	107	262	Gender	2
COMPAS	6172	2	7	7	26	Race	2
DEFAULT	30000	2	23	32	316	Gender	2
ATTRITION	1469	2	34	57	—	Work-life balance	4
LAW	22386	5	5	5	—	Race	2
NURSERY	12960	5	8	8	—	Parents' occupation	3
STUDENT	649	5	32	32	—	Race	2

ATTRITION, LAW, NURSERY, and STUDENT do not require a binary version as they are only run with (Fair)RUG.

## C.2 Further Results on the Comparison of RUG with Proxy PSP and with Exact PSP

Table 9: Results of RUG (h) vs. the exact formulation (e).

	<b>CPU (s)</b>	<b>F1 (%)</b>	<b>Acc. (%)</b>
ADULT	h (7.67)	62.30	83.56
	e (300.00)	58.75	82.67
BANK-MKT	h (3.52)	85.28	85.67
	e (300.00)	80.15	80.79
BANKNOTE	h (0.27)	100.00	100.00
	e (300.00)	99.19	99.27
DIABETES	h (0.16)	44.71	69.48
	e (300.00)	45.00	71.43
HEARTS	h (0.01)	100.00	100.00
	e (207.85)	100.00	100.00
ILPD	h (0.21)	36.62	61.21
	e (300.00)	36.36	63.79
IONOSPHERE	h (0.08)	92.13	90.14
	e (300.00)	92.47	90.14
LIVER	h (0.13)	56.41	50.72
	e (300.00)	62.34	57.97
MAGIC	h (6.01)	89.83	86.33
	e (300.00)	87.99	83.39
MAMMOGRAPHY	h (0.77)	53.16	98.35
	e (300.00)	54.32	98.35
MUSHROOM	h (0.35)	100.00	100.00
	e (300.00)	99.94	99.94
MUSK	h (3.52)	84.70	95.76
	e (300.00)	75.64	93.56
OILSPILL	h (0.15)	37.50	94.68
	e (300.00)	31.58	93.09
PHONEME	h (1.58)	79.75	88.07
	e (300.00)	65.38	81.78
SKINNONSKIN	h (31.16)	99.40	99.05
	e (300.00)	98.69	97.93
TICTACTOE	h (0.28)	98.43	97.92
	e (300.00)	95.97	94.79
TRANSFUSION	h (0.06)	46.15	76.67
	e (300.00)	00.00	76.00
WDBC	h (0.14)	95.12	96.49
	e (300.00)	93.67	95.61
Average scores	h (3,12)	75.64	87.40
	e (294.88)	70.97	86.69

Hyperparameter sets for heuristic: max\_depth = {3,5},  
pen\_par = {0.1,1.0,10.0} and max\_RMP\_calls = {5,15,30}



### C.3 Further Results on Interpretability

Table 10: Results of RUG, FSDT, BinOCT, and CG using five-fold cross validation and grid search for hyperparameter tuning on a hold-out test.

		CPU (s)	F1 (%)	Acc. (%)	NoR	Avg. RL	Avg. NoRpS	Avg. RLpS
ADULT	RUG	9.95	64.09	85.58	18.00	2.44	1.13	2.08
	FSDT	300.00	59.13	83.06	17.00	4.76	1.00	2.86
	BinOCT*	300.00	0.00	75.93	8.00	3.00	1.00	3.00
	CG	300.00	46.30	80.41	4.00	5.00	1.13	5.00
BANK_MKT	RUG	3.90	86.58	86.83	110.00	3.97	9.06	4.03
	FSDT	83.23	77.36	78.64	8.00	3.00	1.00	3.00
	BinOCT*	300.00	0.00	52.62	8.00	3.00	1.00	3.00
	CG	300.00	77.34	77.88	3.00	4.00	1.28	4.00
BANKNOTE	RUG	0.23	100.00	100.00	30.00	2.33	6.62	2.38
	FSDT	3.44	99.17	99.27	25.00	4.76	1.00	4.41
	BinOCT	300.00	97.52	97.82	8.00	3.00	1.00	3.00
	CG	300.00	96.77	97.09	3.00	3.00	1.31	2.46
DIABETES	RUG	0.13	41.46	68.83	21.00	2.62	3.45	2.79
	FSDT	9.99	53.33	72.73	8.00	3.00	1.00	3.00
	BinOCT	300.00	37.50	35.06	8.00	3.00	1.00	3.00
	CG	300.00	50.57	72.08	2.00	4.00	1.09	3.15
HEARTS	RUG	0.03	100.00	100.00	5.00	1.60	2.18	1.39
	FSDT	0.01	100.00	100.00	4.00	2.25	1.00	1.82
	BinOCT	29.47	30.19	39.34	8.00	3.00	1.00	3.00
	CG	0.81	100.00	100.00	2.00	4.00	1.75	4.00
ILPD	RUG	0.13	22.64	64.66	23.00	3.13	2.19	3.31
	FSDT	300.00	39.29	70.69	30.00	8.73	1.00	5.02
	BinOCT	300.00	49.52	54.31	8.00	3.00	1.00	3.00
	CG	300.00	35.71	68.97	2.00	4.00	1.00	4.00
IONOSPHERE	RUG	0.07	95.74	94.37	13.00	2.15	5.01	2.61
	FSDT	300.00	90.53	87.32	13.00	4.38	1.00	4.30
	BinOCT	300.00	31.58	26.76	8.00	3.00	1.00	3.00
	CG	300.00	93.48	91.55	2.00	5.00	1.17	5.00
LIVER	RUG	0.11	56.41	50.72	33.00	3.27	3.87	3.28
	FSDT	300.00	70.59	63.77	31.00	4.97	1.00	4.97
	BinOCT	300.00	58.82	59.42	8.00	3.00	1.00	3.00
	CG	300.00	68.89	59.42	2.00	2.50	1.02	2.21
MAGIC	RUG	5.48	90.17	86.78	125.00	3.90	5.61	3.99
	FSDT	132.74	86.97	82.02	8.00	3.00	1.00	3.00
	BinOCT*	300.00	0.00	35.17	8.00	3.00	1.00	3.00
	CG	300.00	85.00	79.92	3.00	5.00	1.06	5.00
MAMMOGRAPHY	RUG	2.36	70.45	98.84	39.00	2.41	4.09	2.59
	FSDT	4.09	47.22	98.30	8.00	3.00	1.00	3.00
	BinOCT	300.00	30.77	97.99	8.00	3.00	1.00	3.00
	CG	300.00	52.63	98.39	2.00	4.00	1.04	4.00
MUSHROOM	RUG	0.46	100.00	100.00	10.00	2.70	3.70	2.86
	FSDT	0.02	100.00	100.00	13.00	4.08	1.00	3.94
	BinOCT*	300.00	0.00	48.18	8.00	3.00	1.00	3.00
	CG	300.00	95.99	96.00	1.00	4.00	1.00	4.00
MUSK	RUG	1.93	87.77	96.52	61.00	4.18	5.10	4.43
	FSDT	300.00	64.07	90.91	8.00	3.00	1.00	3.00
	BinOCT*	300.00	0.00	84.62	8.00	3.00	1.00	3.00
	CG	300.00	76.79	93.86	4.00	5.00	1.27	5.00
OILSPILL	RUG	0.21	62.50	96.81	32.00	2.66	5.90	2.96
	FSDT	300.00	50.00	96.81	8.00	3.00	1.00	3.00
	BinOCT*	300.00	0.00	95.74	8.00	3.00	1.00	3.00
	CG	300.00	0.00	95.21	2.00	4.00	1.00	4.00
PHONEME	RUG	1.49	77.46	86.86	65.00	3.11	3.82	3.13
	FSDT	300.00	72.96	84.37	32.00	5.00	1.00	5.00
	BinOCT*	300.00	66.98	80.57	8.00	3.00	1.00	3.00
	CG	300.00	63.41	81.31	3.00	4.33	1.20	4.24
SKINNONSKIN	RUG	41.13	99.94	99.91	103.00	2.57	6.95	2.31
	FSDT	300.00	99.14	98.64	25.00	4.76	1.00	4.50
	BinOCT	-	-	-	-	-	-	-
	CG	300.00	95.53	92.83	3.00	2.67	1.33	2.32
TICTACTOE	RUG	0.32	98.04	97.40	35.00	4.20	2.61	4.09
	FSDT	300.00	89.33	85.94	27.00	4.85	1.00	4.51
	BinOCT	300.00	58.13	55.73	8.00	3.00	1.00	3.00
	CG	300.00	90.43	88.54	9.00	3.44	1.63	3.28

Table 10 continued from previous page

		CPU (s)	F1 (%)	Acc. (%)	NoR	Avg. RL	Avg. NoRpS	Avg. RLpS
TRANS-FUSION	RUG	0.06	40.74	78.67	11.00	2.91	0.96	2.82
	FSDT	0.71	48.48	77.33	8.00	3.00	1.00	3.00
	BinOCT	300.00	43.30	63.30	8.00	3.00	1.00	3.00
	CG	300.00	16.67	73.33	2.00	4.50	1.00	4.33
WDBC	RUG	0.11	91.36	93.86	24.00	3.04	5.79	3.19
	FSDT	3.91	86.96	89.47	62.00	7.23	1.00	6.68
	BinOCT*	300.00	95.24	96.49	8.00	3.00	1.00	3.00
	CG	300.00	91.36	93.86	3.00	4.00	1.54	4.59
Average scores	RUG	3.78	76.96	88.15	42.11	2.96	4.11	3.01
	FSDT	163.23	74.14	86.63	18.61	4.27	1.00	3.83
	BinOCT	300.00	35.27	371.08	8.00	3.00	1.00	3.00
	CG	283.38	68.70	85.59	2.89	4.00	1.21	3.92

Hyperparameter sets for RUG: max\_depth = {3,5}, pen\_par = {0.1,1.0,10.0}, max\_RMP\_calls = {5,15,30}.

Hyperparameter sets for FSDT, BinOCT, CG: max\_depth = {3,5,10}.

The time limit was set to 300 seconds. If the time limit was hit we report the solution found within the limit.

- indicates that the method did not return any solution within the time limit.

\* hyperparameter sets excluded some parameters in cases where those lead to execution failure.

**Appendix D. Further Results on the Case Study for Interpretability: Credit Risk Scoring** For this case study we use data from credit risk modelling from the banking industry. We refer to section 4.4 for a detailed account of the data and the measures used to inspect the results.

Following the structure of 4.4, we first focus on interpretability only and fit several ML models to the data, Logistic Regression (LR), Decision Tree (DT), Random Forest (RF), AdaBoost (ADA) (Freund and Schapire, 1997), and LightGBM (Ke et al., 2017) and compare their performances against that of RUG. In all tree-based methods but RF, we set the `maximum-depth` parameter to two. To reach acceptable performance scores with RF, we had to set the same parameter to seven. We report the results in Table 11. We observe that with only three more rules, RUG outperforms a simple decision tree and substantially increases the F1-score from 81.37% (DT) to 87.50% (RUG). With RUG, on average only 1.25 rules are used per sample and thus, RUG can reach higher performance than an interpretable DT while maintaining approximately the same level of global and local interpretability. The F1-score of RUG also exceeds those of RF and LightGBM, both of which produce too many rules to stay interpretable.

Table 11: Case study results of RUG vs. traditional ML models when the focus is on interpretability.

	<b>F1 (%)</b>	<b>Acc (%)</b>	<b>NoR</b>	<b>Avg.RL</b>	<b>Avg.NoRpS</b>	<b>Avg.RLpS</b>
RUG	87.50	97.55	7.00	2.00	1.25	2.00
LR	78.61	96.16	–	–	–	–
DT	81.37	95.65	4.00	2.00	1.00	2.00
RF	85.62	97.37	2163.00	6.87	20.00	7.00
ADA	88.40	97.65	40.00	1.00	20.00	1.00
LightGBM	87.06	97.27	80.00	2.00	20.00	2.00

Avg.RL: Average rule length; NoR: Number of rules; Avg.NoRpS: Average number of rules per sample; Avg.RLpS: Average rule length per sample; \*Maximum depth.

Table 12: Case study results of RUG vs. traditional ML models when the focus is on accuracy.

	<b>F1 (%)</b>	<b>Acc. (%)</b>	<b>NoR</b>	<b>Avg.RL</b>	<b>Avg.NoRpS</b>	<b>Avg.RLpS</b>
RUG	94.68	98.96	44.00	1.98	6.55	2.00
LR	78.61	96.16	–	–	–	–
DT	95.08	99.03	1084.00	12.94	1.00	14.79
RF	95.30	99.07	506181.00	13.36	200.00	13.84
ADA	94.58	98.92	600.00	1.00	300.00	1.00
LightGBM	97.49	99.51	8992.00	4.95	300.00	4.99

Avg.RL: Average rule length; NoR: Number of rules; Avg.NoRpS: Average number of rules per sample; Avg.RLpS: Average rule length per sample; \*Maximum depth.

Second, we attempt to boost performance in terms of accuracy and F1-scores, while keeping a good level of interpretability and report the results in Table 12. Using five-fold cross validation with grid search for hyperparameter tuning, we selected the `maximum-depth` parameter from the set {3,5,7,9,11,15} for the tree-based methods. For RF, ADA and LightGBM, the `number-of-estimators` parameter was chosen from the set {100,150,200,250,300}. With 44 rules, all of length two, RUG seems to maintain a fairly good level of global interpretability while showing competitive performance scores with the other methods, where each tree ensemble method produces more than a thousand rules. Naturally, the DT tree only uses one rule per sample, however, it loses interpretability with an average length of 15.00. Here, RUG yields on average 6.55 rules per sample, each with at most length of two.

Lastly, we report on the implementation of RUG in practice by a large consultancy firm in Istanbul <sup>†</sup>. In Figures 4 and 5 we show screenshots from their user interface (UI) for a

<sup>†</sup>KoçDigital: <https://www.kocdigital.com/en-us/home>

RUG. The RUG output consists of six rules of length two that utilize four of the available 42 features (see Figure 4). The performance of the model is very good, with an accuracy of almost 97% and F1-, precision, and recall scores of at least 85%. Figure 5 displays the prediction and the local explanation of RUG for a single instance. The instance is covered by two rules that make use of only three features. The UI visualizes how the prediction is made, also considering and visualizing the weight of each rule.

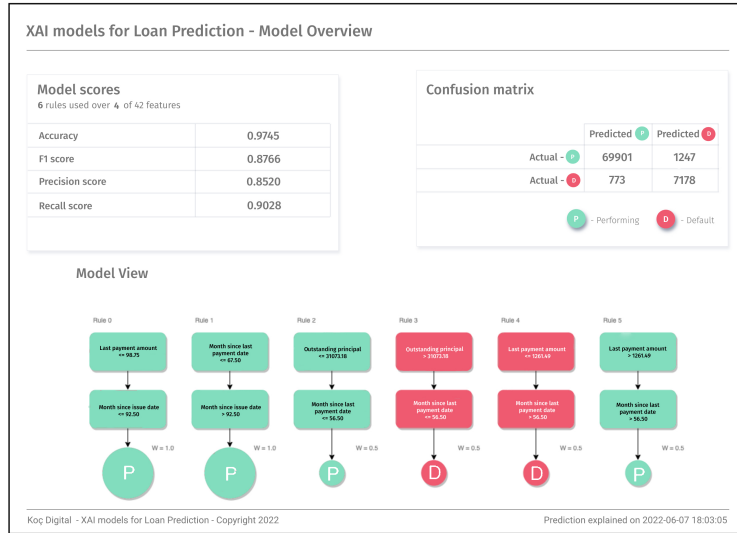


Figure 4: Overview of RUG model trained for loan prediction. The visualization is designed at KoçDigital.

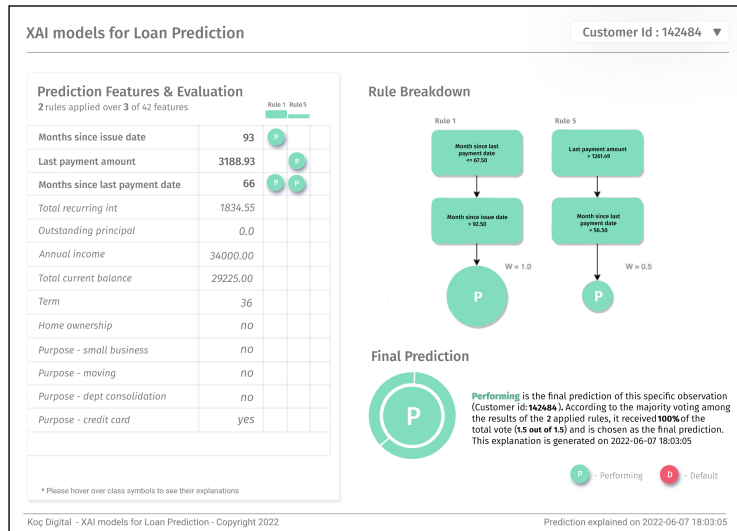


Figure 5: Prediction and local explanation for a single instance using the rules of the trained RUG model. The visualization is designed at KoçDigital.